Plant Science 367 (2026) 113104

Contents lists available at ScienceDirect

Plant Science

journal homepage: www.elsevier.com/locate/plantsci

Inter-plant communication in broccoli (*Brassica oleracea* var. *italica*) through root colonization with the endophytic fungus *Trichoderma hamatum*: New findings in a "wired communication"

Jorge Poveda [a,*], Shiying Qu [a], Pablo Velasco [b,*]

[a] Recognised Research Group AGROBIOTECH, UIC-370 (JCyL), Department of Plant Production and Forest Resources, Higher Technical School of Agricultural Engineering of Palencia, University Institute for Research in Sustainable Forest Management (iuFOR), University of Valladolid, Avda. Madrid 57, Palencia 34004, Spain
[b] Group of Genetics, Breeding and Biochemistry of Brassicas, Mision Biologica de Galicia (MBG-CSIC), Pontevedra 36143, Spain

ARTICLE INFO

Keywords:
Sclerotinia sclerotiorum
Salicylic acid
Jasmonic acid
Glucosinolates
Root-colonization
Plant systemic defenses

ABSTRACT

Inter-plant communication has emerged as a critical yet poorly understood component of plant defense strategies, particularly belowground and beyond mycorrhizal systems. Our work demonstrates that the endophytic fungus *Trichoderma hamatum* mediates effective "wired communication" between neighboring broccoli (*Brassica oleracea* var. *italica*) plants, enhancing resistance against the necrotrophic pathogen *Sclerotinia sclerotiorum*. Using a novel axenic culture system that allows controlled hyphal connections between plant roots, we show that foliar infection of one plant triggers systemic defense priming in an adjacent, non-infected plant, but only in the presence of *T. hamatum*. This inter-plant signaling resulted in a significant reduction of leaf lesion development, increased tissue vitality and reduced oxidative damage in the receiver plant. Mechanistically, fungal-mediated communication was associated with dynamic changes in root colonization patterns rather than with detectable metabolic reprogramming of the fungal mycelium. Defense activation in receiver plants involved strong hormonal rebalancing, characterized by local salicylic acid (SA)–mediated responses in roots and systemic jasmonic acid (JA)–dependent defenses in leaves. Untargeted metabolomics revealed the accumulation of defense-related metabolites, including neoglucobrassicin and lipid-derived compounds linked to SA and JA signaling, in plants that received the fungal-transmitted warning signal. Our findings extend the concept of inter-plant communication to non-mycorrhizal endophytic fungi and identify *T. hamatum* as an active biological conduit for defense signaling in an agriculturally relevant crop. This work highlights fungal-mediated plant connectivity as an ecologically and agronomically relevant mechanism with potential applications in sustainable disease management.

1. Introduction

One of the most significant pathogens impacting plants of the Brassicaceae family is *Sclerotinia sclerotiorum*, a highly aggressive fungus with a broad worldwide distribution. This pathogen is responsible for stem rot in brassica crops and can infect plants through aerial tissues or directly from the soil. Infections caused by *S. sclerotiorum* lead to substantial yield losses, reaching as much as 80% of global annual losses in rapeseed production (Hossain et al., 2023; Shang et al., 2024). Current approaches to disease control involve agronomic practices such as crop rotation, lowering planting density, residue burning, and irrigation to promote sclerotia degradation; the development and use of resistant cultivars through conventional or molecular breeding; application of chemical fungicides including anilinopyrimidines, methyl-benzimidazole carbamates and dicarboxamides; as well as biological control using bacterial agents (*Bacillus* spp., *Streptomyces* spp.), fungal antagonists (*Coniothyrium minitans*, *Trichoderma* spp.) and mycovirus-based biological control agents (BCAs) (O'Sullivan et al., 2021).

The fungal genus *Trichoderma* is among the most extensively researched and commonly applied BCAs in agriculture, owing to its wide distribution across a variety of ecosystems and climatic zones (Afzal et al., 2021). Species belonging to this genus function as efficient biofertilizers by stimulating plant growth through nutrient solubilization and chelation (including P, Fe, Mg and Mn), the synthesis of phytohormones, such as auxins, and the regulation of rhizospheric microbial

* Corresponding authors.
E-mail addresses: jorge.poveda@uva.es (J. Poveda), pvelasco@mbg.csic.es (P. Velasco).

https://doi.org/10.1016/j.plantsci.2026.113104
Received 12 January 2026; Received in revised form 20 February 2026; Accepted 10 March 2026
Available online 11 March 2026

communities (Gupta, 2020). In addition, several *Trichoderma* species improve plant resilience to abiotic stresses by reducing oxidative damage, modulating gene expression, and directly participating in the mycoremediation of pollutants and heavy metals (dos Santos et al., 2022). Nevertheless, the main agricultural relevance of *Trichoderma*--based bioinoculants resides in their application as biological control agents, representing up to 60% of the biofungicides currently available on the global market (Kubiak et al., 2023).

The biological control activity of *Trichoderma* species is mediated through multiple mechanisms, including mycoparasitism, antibiosis, competition for nutrients and ecological niches, and the induction of plant defense responses (Guzmán-Guzmán et al., 2023). These fungi are capable of triggering both localized and systemic defense pathways in plants. Host recognition of *Trichoderma*-derived microbe-associated molecular patterns (MAMPs) activates complex signaling networks regulated by defense-related phytohormones, primarily salicylic acid (SA), jasmonic acid (JA) and ethylene (ET). As a result, plants increase the production and accumulation of antimicrobial proteins and secondary metabolites, thereby strengthening resistance against subsequent pathogen challenges (Khan et al., 2023). Recently, *Trichoderma*'s ability to actively release pathogen-associated molecular patterns (PAMPs) from the cell walls of pathogens has also been described, which also act as elicitors of plant defenses (Velasco et al., 2026). Specifically, *Trichoderma hamatum* has recently been the focus of a dedicated review that emphasizes its wide range of functional traits, such as its ability to enhance plant growth, exert antimicrobial and antioxidant effects, display insecticidal and herbicidal activities, and contribute to mycoremediation processes (Lodi et al., 2023).

Although *Trichoderma* is able to perform several plant-beneficial functions while inhabiting the rhizosphere, the expression of many of these effects requires its establishment as a root endophyte. Root colonization by *Trichoderma* is typically restricted to the outer root tissues and does not extend into the vascular system, as plants activate localized defense responses mediated by SA and callose deposition. This controlled defense limits fungal spread and prevents *Trichoderma* from adopting a systemic pathogenic lifestyle, thereby allowing a stable and beneficial interaction to be maintained (Alonso-Ramírez et al., 2014; Pozo et al., 2024).

The capacity of plants to release and perceive chemical signals that enable communication among individuals has become an increasingly explored research area in recent decades. Plant-to-plant signaling was first documented in 1983, when studies showed that mechanical leaf damage caused by herbivores in willows and poplars triggered the emission of chemical cues from the affected plants, which in turn activated defense responses in neighboring plants (Baldwin and Schultz, 1983; Rhoades, 1983). The first comprehensive review on this topic appeared in 2000, emphasizing the role of SA and JA derivatives as volatile organic compounds (VOCs) mediating communication between plants following herbivore or pathogen attacks (Agrawal, 2000). More recently, multiple mechanisms of inter-plant signaling have been characterized, including VOC emission, electrical and acoustic signals in aerial tissues and, belowground, the involvement of root exudates, direct root contact and hyphal networks (Sharifi and Ryu, 2021; Singh and Satheeshkumar, 2025).

In terms of inter-plant communication via hyphal networks, one of the most widely recognized phenomena involves mycorrhizal fungi forming common mycorrhizal networks (CMNs), which enable forest trees to exchange information in a manner often likened to a natural "internet" (Simard, 2018). This phenomenon has opened a new avenue of study, giving rise to what researchers have begun to call inter-plant "wired communication" (Boyno and Demir, 2022). These CMN-mediated connections can occur even between distantly related plant species, including herbaceous plants and trees (Gilbert and Johnson, 2017). Both chemical signaling molecules and electrical signals may participate in this communication, enhancing plant chemical defenses against biotic and abiotic stresses and potentially facilitating collective neural-like interactions among plants (Johnson and Gilbert, 2015; Simard, 2018). In contrast, the role of filamentous endophytic fungi as mediators of inter-plant communication, through simultaneous colonization of the rhizosphere and roots, remains largely unexplored (Oelmüller, 2019). Notably, one study demonstrated that colonization of *Arabidopsis thaliana* roots by the endophytic fungus *Piriformospora indica* can mediate communication to neighboring plants following leaf infection by the pathogen *Alternaria brassicae*. The infection triggered a JA-dependent systemic resistance in the host plant, which was transmitted via *P. indica* hyphae to surrounding plants, where it was converted into an abscisic acid (ABA)-mediated defense response (Vahabi et al., 2018). Subsequently, we described the ability of *T. hamatum* to act as a communicator between *A. thaliana* plants through root colonization of neighboring plants. Specifically, *T. hamatum* was able to induce JA-mediated defenses in the neighboring plant when the first plant was infected foliarly by *S. sclerotiorum* (necrotrophic pathogen). This defensive induction did not occur if the plant was foliarly infected by a hemibiotrophic pathogen, such as the bacterium *Xanthomonas campestris* (Poveda et al., 2023a). Consequently, inter-plant signaling through fungal networks, especially involving non-mycorrhizal fungi, represents a largely untapped research area (Rillig et al., 2025).

In this context, the main objective of this study is to further investigate communication between neighboring plants mediated by *T. hamatum*, using broccoli as a model plant, *S. sclerotiorum* as a leaf pathogen, and a novel plant and fungal culture system. This system allowed us to control root colonization by *T. hamatum* mycelium under axenic conditions, as well as to collect samples from different plant organs and mycelium in order to analyze defensive gene expression and possible metabolic changes.

This study substantially expands our previous work conducted in *A. thaliana* (Poveda et al., 2023a). While that study demonstrated that *T. hamatum* could mediate inter-plant communication under a simplified *Arabidopsis* model, it did not address whether this mechanism operates in an agriculturally relevant crop, nor did it characterize the underlying metabolic adjustments in either the fungus or the plant. In contrast, the present work establishes a novel axenic two-plant culture system specifically adapted to broccoli and provides, for the first time, a mechanistic analysis of fungal-mediated communication in a crop species. This includes quantification of fungal colonization dynamics, plant hormonal responses, and untargeted metabolomics in roots, leaves, and interconnecting fungal mycelium. Therefore, this manuscript not only validates fungal "wired communication" in a real crop but it also allows for the analysis of aspects that were impossible in the previous system with *A. thaliana* and soil, such as fungal metabolomics, making it possible to confirm or rule out how the fungus is able to communicate with the two neighboring plants.

2. Material and methods

2.1. Biological material

Broccoli (*Brassica oleracea* var. *italica*) was used as the model plant for this study, as it is a crop that has been growing in scientific interest in recent years due to its status as a "superfood" because of its content of glucosinolates (mainly sulforaphane) and selenium (Han et al., 2021). The plant used in the study was the double haploid inbred line of broccoli "Early Big", in order to obtain the lowest possible variability in plant responses to the different treatments. Seeds were obtained from the MBG's crop brassica germplasm bank.

T. hamatum was previously isolated from the roots of kale (*B. oleracea* var. *acephala*) in Galicia, northwestern Spain, where it was found to induce systemic resistance against foliar attacks by the phytopathogenic bacterium *Xanthomonas campestris* (Poveda et al. 2020) and a biostimulant that promotes plant growth and the accumulation of glucosinolates and antioxidants in the leaves (Velasco et al., 2021). The plant-pathogen used in the study was the necrotrophic fungus *S.*

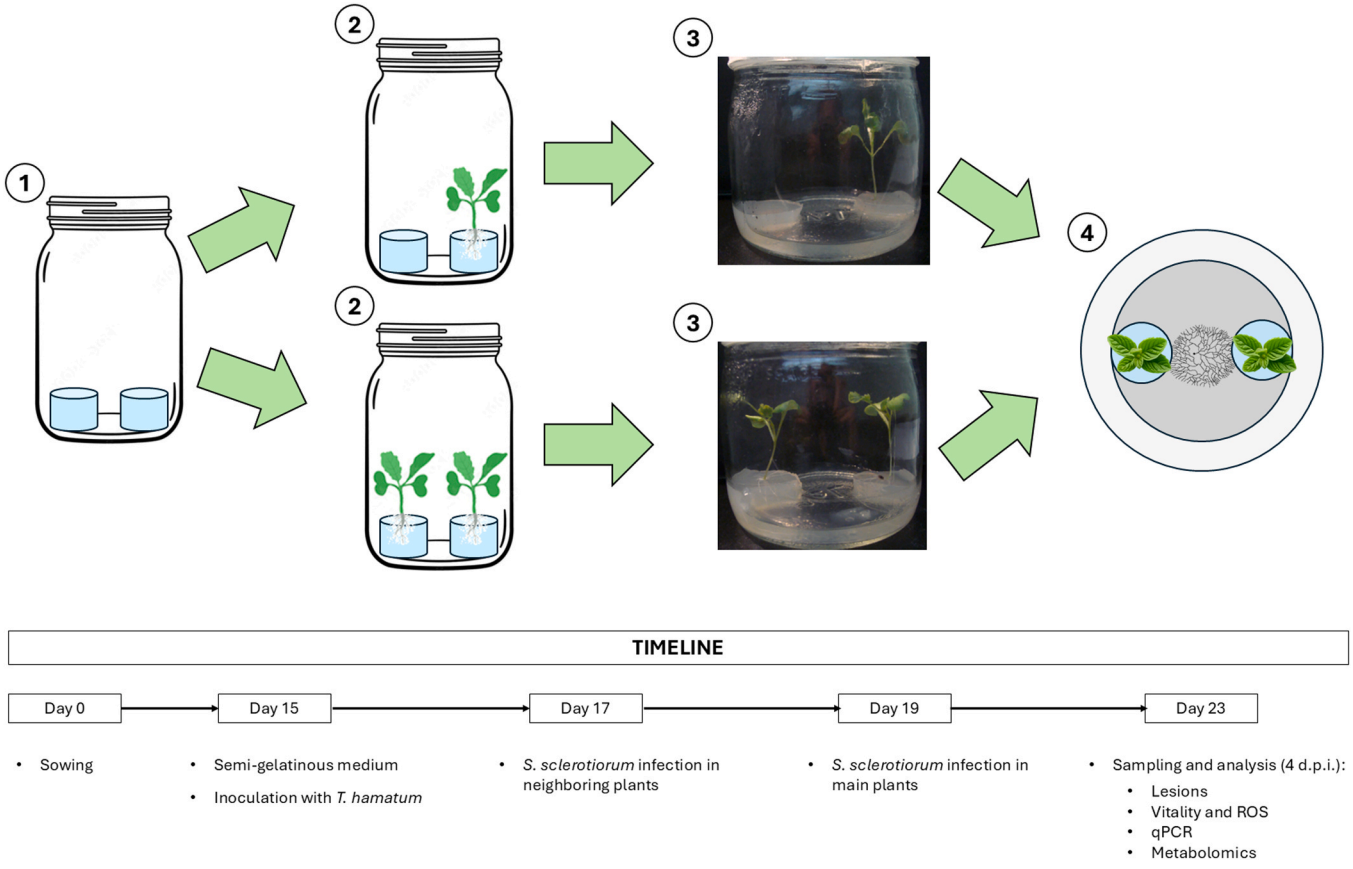

Fig. 1. Graphical representation of the axenic culture methodology in "islands" with broccoli seedlings. 1) Representation of the agar "islands" in the glass flasks. 2) Representation of seedling growth in one of the two islands and in the two islands of each flask. 3) Photographs of the flasks with 15-day-old broccoli seedlings growing in the "islands" and the gel-like consistency medium applied in the space between the "islands". 4) Growth of *Trichoderma* connecting the "islands" 48 h after inoculation.

sclerotiorum (Ss) isolate MBG-Ss2, collected from a naturally infected plant of rapeseed (*B. napus*) in an experimental field at Misión Biológica de Galicia (MBG-CSIC). The fungus was routinely cultivated on potato dextrose agar (PDA, Sigma-Aldrich, Madrid, Spain) in darkness at 28 °C. Spores were harvested from 7-day-old PDA dishes as previously described by Morcuende et al. (2024).

2.2. Plant growth, Trichoderma inoculation and S. sclerotiorum foliar infections

A new *in vitro* culture methodology was developed using plants and fungi to obtain *T. hamatum* mycelium that connected the roots of two neighboring broccoli plants. First, an axenic culture was established with broccoli seeds in a similar manner to that previously performed in magenta boxes with *A. thaliana* seeds (Poveda et al., 2023b). Broccoli seeds were surface sterilized by vigorous shaking in 70% ethanol and 1% Triton X-100 solution for 20 min, followed by washing with 2.5% sodium hypochlorite and 0.005% Triton X-100 solution for 10 min.

The containers used for axenic culture were 0.5 L glass flasks (Vicasa, Madrid, Spain). These flasks were filled with 100 mL of Murashige and Skoog (MS) (Duchefa, Haarlem, Netherlands) (4.41 g/L) solid medium (agar 10 g/L) with sucrose (30 g/L). In the solid growth medium, one or two (depending on the number of plants cultivated) "islands" of 3 cm in diameter were "carved" using sterile spoons, located at opposite ends of the jar (Fig. 1). Therefore, when there were two "islands" of MS medium, the separation between them was 4 cm. A broccoli seed was placed on each of the "islands." The purpose of the system is for the seedling to grow and the roots to colonize a localized volume (the "island"). Once the seeds were deposited on the "islands," the flasks were sealed with

Table 1
Codes used for the different conditions of the experiments and analyses.

CODE	DESCRIPTION
1 P	A single plant without *T. hamatum* inoculation and without pathogenic infection.
2 P	Two neighboring plants without *T. hamatum* inoculation and without pathogenic infection.
1 P+Th	A single plant with *T. hamatum* inoculation and without pathogenic infection.
2 P+Th	Two neighboring plants with *T. hamatum* inoculation and without pathogenic infection.
1 P+Ss	A single plant without *T. hamatum* inoculation and foliar infected with *S. sclerotiorum*.
2 P+Ss-o	Two neighboring plants without *T. hamatum* inoculation and foliar infected with *S. sclerotiorum*, without neighbor plant infected 48 h before.
2 P+Ss-w	Two neighboring plants without *T. hamatum* inoculation and foliar infected with *S. sclerotiorum*, with neighbor plant infected 48 h before.
2 P+Ss-w-np	It refers specifically to the neighboring plant infected 48 h before its neighbor.
1 P+Th+Ss	A single plant with *T. hamatum* inoculation and foliar infected with *S. sclerotiorum*.
2 P+Th+Ss-o	Two neighboring plants with *T. hamatum* inoculation and foliar infected with *S. sclerotiorum*, without neighbor plant infected 48 h before.
2 P+Th+Ss-o-np	It refers specifically to the neighboring plant non-infected 48 h before its neighbor.
2 P+Th+Ss-w	Two neighboring plants with *T. hamatum* inoculation and foliar infected with *S. sclerotiorum*, with neighbor plant infected 48 h before.
2 P+Th+Ss-w-np	It refers specifically to the neighboring plant infected 48 h before its neighbor.

Table 2
Primers used in this work.

Code	Sequence (5′−3′)	Use	Reference
Act-T-F	ATGGTATGGGTCAGAAGGA	Endogenous *Trichoderma* gene	Velasco et al. (2021)
Act-T-R	ATGTCAACACGAGCAATGG		
Act-Boi-F	TTCAAGCTGGAGCCAAGAAGGTTC	Endogenous broccoli gene	Liu et al. (2024)
Act-Boi-R	ACGAATGGTGCGAGACAGTTAGTG		
PAL-Boi-F	AGCAGCGGAACAGATGAA	Phenylalanine ammonia lyase (gene related to SA synthesis)	Guo et al. (2023)
PAL-Boi-R	ACTCCCTTTCATCTGTTCC		
PR-1-Boi-F	GCGACTGCAGACTCGTACAC	Pathogenesis related 1 (gene related to SA response)	Lovelock et al. (2013)
PR-1-Boi-R	TCTCGTTGACCCAAAGGTTC		
AOS-Boi-F	GAATCCGTAAATACAACTCCACAG	Allene oxide synthase (gene related to JA synthesis)	Torres-Contreras et al. (2018)
AOS-Boi-R	CTCGACCTTATCAACATCGAACAA		
OPR1-Boi-F	CACCGTCAACGACCGAACT	12-Oxophytodienoate reductase 1 (gene related to JA response)	Fang et al. (2020)
OPR1-Boi-R	TGAGGCTCTGTATCTCCCGACT		

adhesive tape (3 M Micropore, Bracknell, UK) and kept in a growth chamber at 22 °C, 40% relative humidity (RH), and a 16 h light/8 h dark photoperiod at 80–100 μE m^2/s.

After 15 days of plant growth, inoculation with *T. hamatum* was carried out. In all flasks, 20 mL of MS medium with less agar (3 g/L) was applied in order to obtain a gel-like consistency (Fig. 1). In the flasks treated with *T. hamatum*, 1 μL with 10^7 conidia was applied in the center. After 48 h in the growth chambers, the mycelium of *T. hamatum* had come into contact with the roots of the plants in the flasks (Fig. 1).

At that point, foliar infection with the pathogen *S. sclerotiorum* in "neighboring plants" was carried out, according to the methodology described above by Poveda et al. (2023a). The mycelium grown in three PDA Petri dishes was harvested and transferred into a Falcon tube containing 30 mL of sterile distilled water. To this, 0.5 g of Ballotini glass beads (0.15–0.25 mm in diameter) and another 0.5 g of beads with a 1 mm diameter (Potters, Saint-Pourçain-sur-Sioule, France) were added. The mixture was then vigorously shaken for 20 min. The resulting mycelial suspension was adjusted to an absorbance of 0.17 at 520 nm per mL, and 1 μL was used to infiltrate the leaves. To assess the impact of pre-infecting a neighboring plant, one of the two plants sharing the same flask was inoculated 48 h prior to infecting the remaining plants, as specified. All the codes used throughout the work for the different conditions are summarized in Table 1. Each treatment was established using 20 flasks, resulting in a total of 80 flasks for the four single-plant treatments (4 different treatments) and 120 flasks for the six two-plant treatments (6 different treatments). From these, 17 flasks per treatment were subsequently used for destructive sampling and downstream analyses. The complete assay was repeated twice.

2.3. Pathogen effect analysis

2.3.1. Injuries measurement

Photographs of each of the 20 infected leaves per treatment were taken 4 days after infection (d.p.i.). Lesion areas on the leaves were measured using ImageJ software (developed by the U.S. National Institutes of Health, Bethesda, MD, USA).

From the 20 leaves collected for each condition, 12 were grouped into four sets of three leaves each, then flash-frozen in liquid nitrogen and ground using a mortar and pestle. The remaining 8 leaves were reserved for further analysis described in Sections 2.3.2 and 2.3.3.

From 12 flasks of each different treatment (1 or 2 plants, with or without *T. hamatum*, with or without infection by the pathogen, and with or without previous infection of the neighboring plant by the pathogen), the entire aerial part and root system were collected separately, as well as the mycelium of *T. hamatum*, were washed with sterile distilled water and rapidly frozen in liquid nitrogen. Part of the aerial part was separated and crushed with a mortar and liquid nitrogen, together with part of the roots, for nucleic acid analysis (Section 2.4. and 2.6.). The rest of the tissues were freeze-dried and ground for biochemical analysis (Section 2.5.).

Therefore, all plant and fungal samples collected for subsequent biochemical, transcriptomic, and metabolic analyses were taken 4 d.p.i. with the pathogen. In plants not infected with *S. sclerotiorum*, samples were taken at exactly the same time point.

2.3.2. Vitality test in tissues

The vitality assessment of *broccoli* leaves was performed following the protocol described by Poveda (2022). This method relies on the ability of living tissue to reduce triphenyltetrazolium chloride (TTC) into red-colored, insoluble triphenylformazan (TF), a process linked to mitochondrial respiratory chain activity. Only viable cells are capable of carrying out this reduction. For the assay, 100 mg of fresh tissue from 8 leaves was placed in 1 mL of 1% TTC solution and incubated at 37 °C for 72 h. After incubation, 200 mg of Ballotini glass beads (ranging from 0.15 to 0.25 mm to 1 mm in diameter) were added to each 1.5 mL Eppendorf tube. Samples were vigorously vortexed, then centrifuged at 10,000 rpm for 15 min. The supernatant was discarded, and 1 mL of isopropanol was added to extract the TF. After a second round of vortexing and centrifugation under the same conditions, the resulting supernatant was collected to measure absorbance at 620 nm, which served as an indirect indicator of tissue vitality in broccoli leaves.

2.3.3. Indirect quantification of reactive oxygen species (ROS) in tissues

Reactive oxygen species (ROS) were indirectly quantified using the method described by Poveda (2020), based on measuring electrolyte leakage as an indicator of oxidative damage in plant tissues. This approach relies on the fact that increased ROS production compromises membrane integrity, leading to ion leakage. To perform the assay, 8 fresh leaves were used, and 1 cm^2 sections of tissue were placed briefly in water, then floated in 5 mL of double-distilled water at room temperature for six hours. The initial conductivity of the surrounding water was measured using a Crison™ MM41 pH/conductivity meter (Crison, Barcelona, Spain), representing the electrolyte loss from the tissue (Reading 1). Subsequently, the samples were boiled at 90 °C for 20 min. Once cooled, conductivity was measured again to determine the total ion content of the tissue (Reading 2). The percentage of electrolyte leakage, serving as an indirect indicator of ROS levels, was calculated using the formula: (Reading 1 / Reading 2) × 100.

2.4. Quantification of Trichoderma-root colonization

In the root pools (4 pools with 3 root systems each) from the flasks inoculated with *T. hamatum*, root colonization was quantified by qPCR, using the methodology previously described by Velasco et al. (2021), with modifications. Genomic DNA was isolated from the roots of *T. hamatum*-inoculated plants using the Phire Plant Direct PCR Kit (Thermo Fisher Scientific, Waltham, MA, USA). PCR reactions were set up in a total volume of 10 μL, consisting of 5 μL of Brilliant SYBR Green QPCR Master Mix (Roche, Penzberg, Germany), 10 ng of template DNA, forward and reverse primers at a final concentration of 100 nM, and nuclease-free, PCR-grade water to complete the volume. The *Actin* gene was used as an endogenous reference for both broccoli and *Trichoderma*

(Table 2). Amplifications were carried out on an ABI PRISM 7000 Sequence Detection System (Applied Biosystems, Foster City, CA, USA) under the following thermal cycling conditions for 40 cycles: denaturation at 95 °C for 15 s, annealing at 60 °C for 1 min, and extension at 72 °C for 1 min. Each PCR was performed in triplicate using DNA extracted from four pooled root samples, each pool consisting of roots from three plants per treatment. Cycle threshold values were used to quantify the amount of fungal DNA based on standard curves generated with ten known concentrations of *Trichoderma* DNA and their corresponding Ct values for the *Actin* gene. Fungal DNA levels were normalized to the amount of plant DNA present in each corresponding sample.

2.5. Metabolite profiling

In the mycelium pools (4 pools with 3 complete mycelia each) from the flasks inoculated with *T. hamatum*, an untargeted metabolomic study was performed. The aim was to determine whether possible metabolic changes in *Trichoderma* were related to the reported results of plant defense induction. Metabolite analysis was performed using the methodology previously described by Lana et al. (2023), with modifications. For analysis, 50 mg of freeze-dried mycelial powder were extracted with 500 mL of 80% aqueous methanol and subjected to sonication for 15 min. The resulting extracts were centrifuged at 16,000 ×g for 10 min at room temperature, after which the supernatants were filtered through a 0.20 µm PTFE membrane and collected in vials for subsequent analysis.

Metabolomic profiling was carried out using ultra-performance liquid chromatography coupled to electrospray ionization quadrupole time-of-flight tandem mass spectrometry (UPLC–ESI–QTOF–MS/MS). Analyses were performed on a Thermo Dionex Ultimate 3000 liquid chromatography system (Thermo Fisher Scientific, Waltham, MA, USA) interfaced with a Bruker Compact™ mass spectrometer fitted with a heated electrospray ionization source. Separation of metabolites was achieved on an Intensity Solo 2 C18 column (2.1 × 100 mm, 1.7 µm; Bruker Daltonics, Billerica, MA, USA) employing a binary solvent gradient consisting of 0.1% formic acid in water (mobile phase A) and acetonitrile (mobile phase B).

The chromatographic gradient was programmed as follows: 3% solvent B from 0 to 4 min; a linear increase from 3% to 25% B between 4 and 16 min; a further rise from 25% to 80% B from 16 to 25 min; an increase to 100% B between 25 and 30 min; an isocratic hold at 100% B until 32 min; a return to 3% B from 32 to 33 min; and re-equilibration at 3% B until 36 min. The injection volume was 5 µL, with a flow rate of 0.4 mL/min and the column temperature maintained at 35 °C. Mass spectra were recorded over an m/z range of 50–1200. Data acquisition was carried out in both positive and negative electrospray ionization modes using the following parameters: gas flow rate of 9 L/min, nebulizer pressure of 38 psi, dry gas flow of 9 L/min, and a dry gas temperature of 220 °C. The capillary voltage was set to 4500 V, and the end plate offset was 500 V.

External mass calibration was carried out by direct infusion of a 1 mM sodium formate/acetate solution prepared in a 50:50 (v/v) mixture of isopropanol and water containing 0.2% formic acid. Prior to sample analysis, instrument performance and stability were assessed through three consecutive injections of chloramphenicol (ESI–; ΔRT = 0.02 min; $\Delta m/z = 0.002$) and triphenyl phosphate (ESI+; ΔRT = 0.02 min; $\Delta m/z = 0.001$). A calibration standard was injected at the start of each analytical batch, and all acquired spectra were calibrated prior to statistical evaluation.

MS/MS analyses were conducted based on previously established accurate mass values and retention times, using collision energy ramps between 15 and 50 eV. Feature detection and alignment, along with the construction of bucket tables for both positive and negative ionization modes, were performed using the T-Rex 3D algorithm implemented in MetaboScape 4.0 (Bruker Daltonics, Billerica, MA, USA). Tentative identification of significant metabolites was performed by matching accurate mass values and MS/MS fragmentation spectra against public databases, including PubChem, ChEBI, HMDB, Coconut, Supernatural, etc. by using the software Sirius 6.3.1 (https://bio.informatik.uni-jena.de/sirius/) (Dührkop et al., 2019).

On the other hand, an untargeted metabolomics analysis was also performed on the plant pools (4 pools with 3 root systems or aerial parts each). In this case, the objective was to determine the defensive metabolites possibly involved in the previously reported results of root colonization by *T. hamatum* and leaf infection by *S. sclerotiorum*. The same extraction and analysis procedure described above was followed, also starting with 50 mg of freeze-dried powder.

2.6. Defense-genes expression analysis

Gene expression analysis by RT-qPCR was performed on the four pools of three broccoli plants (aerial parts or roots) that were not freeze-dried (described in Section 2.3.1), using the methodology described by Poveda et al. (2022), with modifications. Total RNA was extracted from 100 mg of pooled tissue samples using the Spectrum™ Plant Total RNA Kit (Qiagen, Valencia, CA, USA). Residual genomic DNA was eliminated by treating the RNA preparations with RQ1 RNase-Free DNase (Promega, CA, USA) according to the manufacturer's protocol. First-strand cDNA was synthesized from 1 µg of total RNA using the GoScript™ Reverse Transcription System (Promega, Madison, WI, USA), following the supplier's instructions. RT-qPCR was performed on a 7500 Real-Time PCR System (Applied Biosystems, Foster City, CA, USA) using a Promega reagent kit in a final reaction volume of 15 µl. The amplification protocol consisted of an initial denaturation step at 95 °C for 10 min, followed by 40 cycles of denaturation at 95 °C for 15 s and annealing/extension at 60 °C for 60 s. All reactions were conducted in triplicate. Threshold cycle (Ct) values were normalized against the broccoli *Actin* gene, which served as the internal reference. Primer sequences used for amplification of *phenylalanine ammonia lyase* (*PAL*) (gene related to SA synthesis), *pathogenesis-related 1* (*PR-1*) (gene related to SA response), *allene oxide synthase* (*AOS*) (gene related to JA synthesis) and *12-oxophytodienoate reductase 1* (*OPR1*) (gene related to JA response) are listed in Table 2. Relative gene expression levels were calculated using the $2^{-\Delta\Delta Ct}$ method (Livak and Schmittgen, 2001).

2.7. Statistical analysis

Statistical analyses were performed using Statistix 8.0 software. To evaluate the combined impact of *Trichoderma* inoculation and the presence of a neighboring plant, a two-way ANOVA was conducted, followed by Sidak's post hoc test for multiple comparisons. Distinct letters denote statistically significant differences at $p < 0.05$. For pairwise comparisons, a one-way ANOVA was applied along with Tukey's multiple range test, with different letters indicating significant differences ($p < 0.05$).

Statistical evaluation of the metabolomic data was performed using the web-based tool MetaboAnalyst (Chong et al., 2019). Variables lacking relevant information were excluded by applying an interquartile range (IQR) filtering step. Quality control samples were used to remove variables that show a coefficient of variance higher than 25%. In addition, Pareto scaling was employed to minimize systematic offsets and to equilibrate the contribution of ions across different abundance levels. The processed data were organized into a three-dimensional matrix (features, samples and variables) and subsequently used for downstream statistical analyses.

In mycelium and plant metabolomic analysis, differentially accumulated metabolites were additionally identified using the Volcano Plot method, which simultaneously integrates *t*-test statistics and fold-change values. Metabolites exhibiting an absolute $\log_2$ fold change of at least 1 and a statistically significant difference between mycelia or plants (FDR ≤ 0.05) were selected as significant.

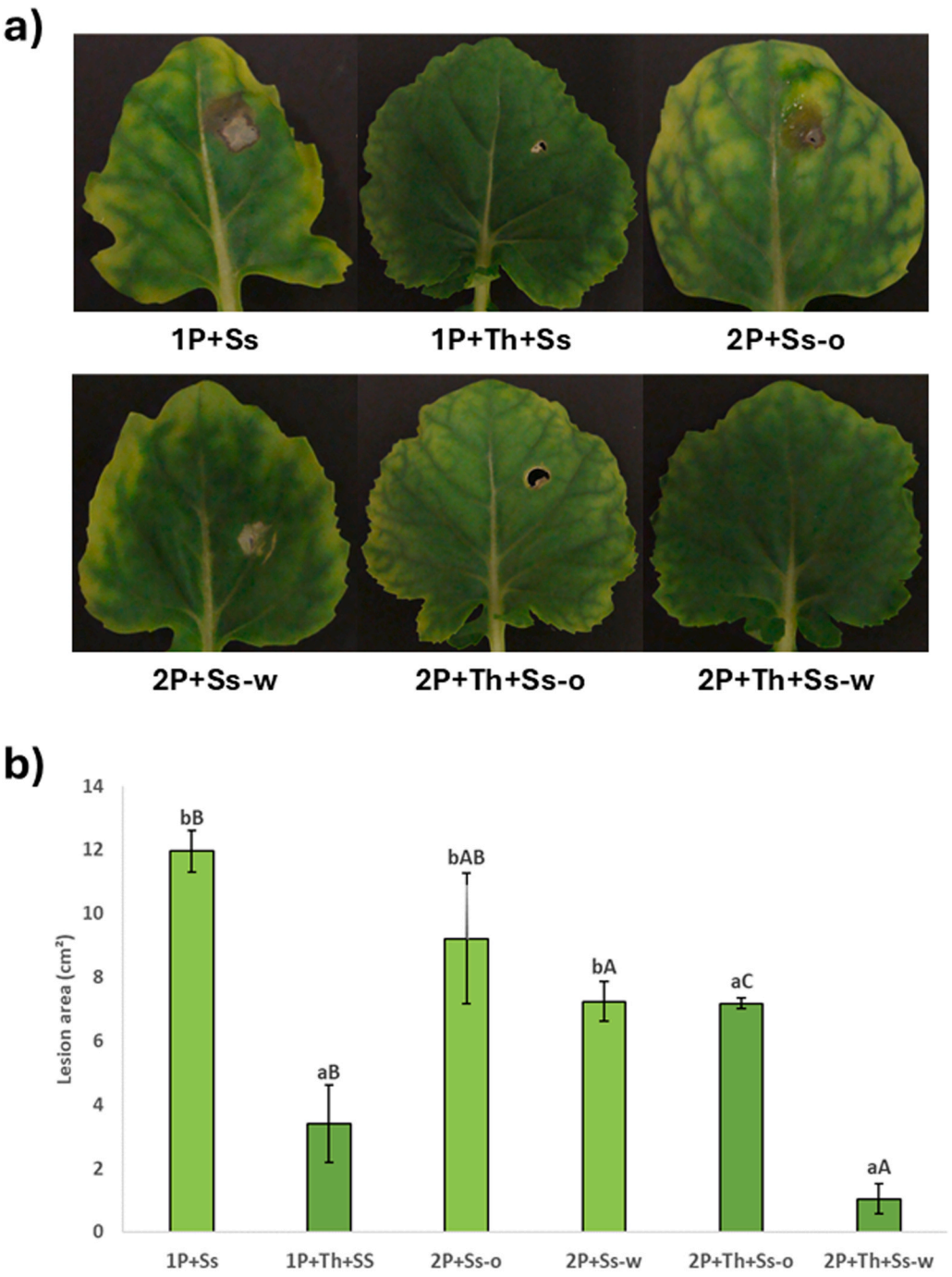

Fig. 2. Broccoli leaves Ss-infected (+Ss) (a) and lesions area quantification (mm^2) (b). One plant (1 P) or two neighboring plants (2 P) were used. Data are the mean of 20 leaves for each condition. Two-way analysis of variance (ANOVA) was performed, followed by Sidak's multiple comparison test. Different letters represent significant differences ($p < 0.05$), for *T. hamatum* inoculation (+Th) (identify by small letters) and for presence of infected neighboring plant (w) (identify by capital letters).

3. Results

3.1. *S. sclerotiorum* foliar infections

Broccoli leaf lesions caused by *S. sclerotiorum* when the flasks contained a single plant were significantly lower when the plants were root inoculated with *T. hamatum* (1 P+Th+Ss: 3.40 ± 1.20 cm^2), compared to plants without this inoculation (1 P+Ss): 11.96 ± 0.66 cm^2) (Fig. 2). In flasks with two plants, without *Trichoderma* inoculation, there were no differences between plants whose neighbor had been pre-infected with *S. sclerotiorum* 48 h earlier (2 P+Ss-w: 7.24 ± 0.63 cm^2), compared to plants without this pre-infection of the neighboring plant (2 P+Ss-o: 9.21 ± 2.05 cm^2). When *T. hamatum* was inoculated in these flasks with two plants, the area of the lesion caused by *S. sclerotiorum* was significantly smaller in plants whose neighbor had been pre-infected 48 h earlier (2 P+Th+Ss-w: 1.08 ± 0.48 cm^2), compared to plants whose neighbor had not been pre-infected (2 P+Th+Ss-o: 7.18 ± 0.18 cm^2) (Fig. 2).

With regard to the vitality of broccoli leaves, when the flasks contained a single plant, the leaves had significantly greater vitality after infection with *S. sclerotiorum* in the presence of *Trichoderma* (1 P+Th+Ss: 0.078 ± 0.018) than in its absence (1 P+Ss: 0.035

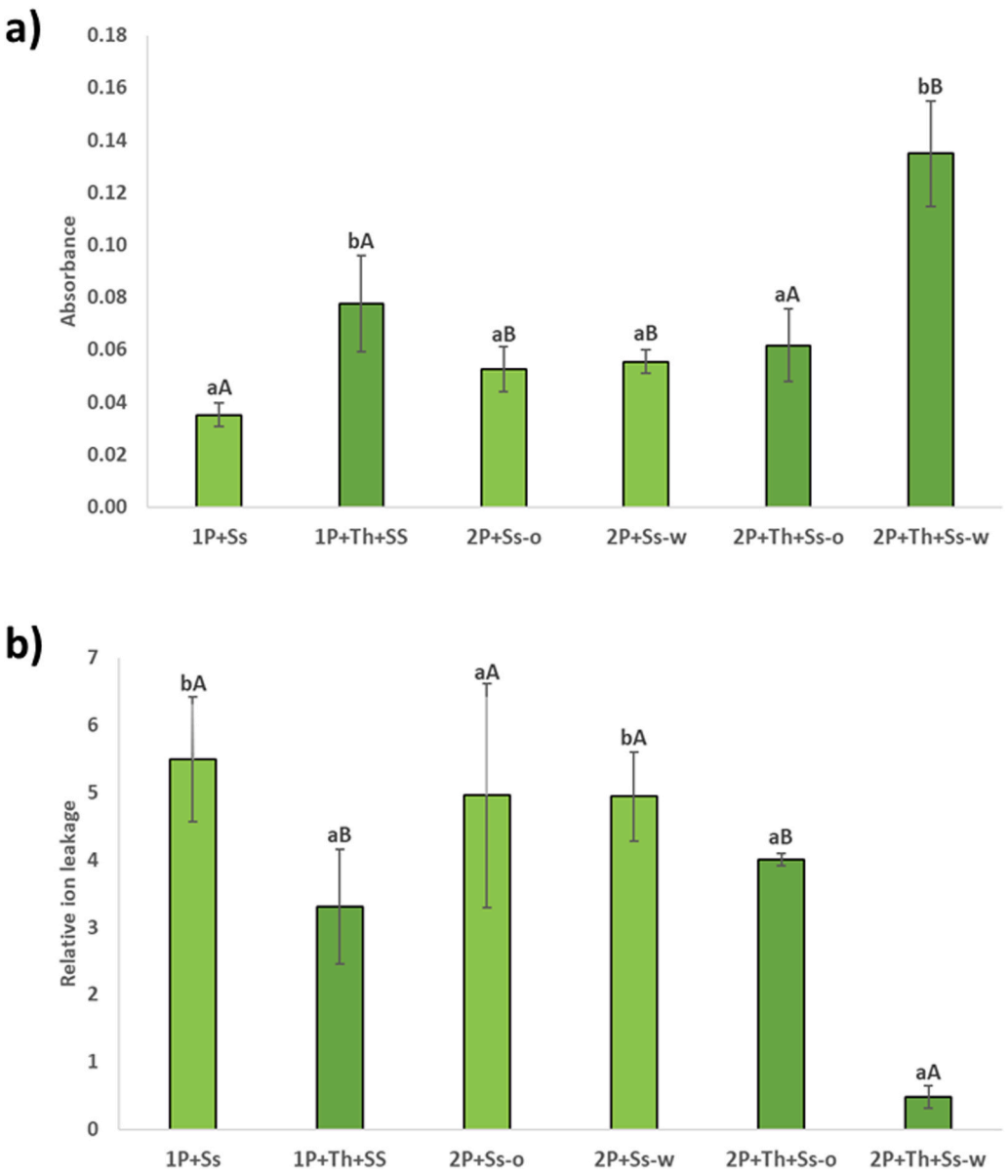

Fig. 3. Tissue vitality by TTC test (a) and indirect quantification of ROS (b) in broccoli leaves Ss-infected (+Ss), where the absorbance at 620 nm (TTC test) and the relative ion leakage (indirect ROS measurement) were analyzed. One plant (1 P) or two neighboring plants (2 P) were used. Data are the mean of 8 leaves for each condition. Two-way analysis of variance (ANOVA) was performed, followed by Sidak's multiple comparison test. Different letters represent significant differences ($p < 0.05$), for *T. hamatum* inoculation (+Th) (identify by small letters) and for presence of infected neighboring plant (w) (identify by capital letters).

± 0.004) (Fig. 3a). When the flasks contained two plants, there were no significant differences in the vitality of the leaves of plants whose neighboring plant had not been pre-infected 48 h earlier, whether *T. hamatum* was present (2 P+Th+Ss-o: 0.062 ± 0.014) or not (2 P+Ss-o: 0.053 ± 0.009). However, when the neighboring plant had been pre-infected 48 h earlier, a significant increase in leaf cell vitality was reported in the second plant when *Trichoderma* was present (2 P+Th+Ss-w: 0.135 ± 0.02), compared to the same plants in the absence of the endophyte (2 P+Ss-w: 0.055 ± 0.004) (Fig. 3a).

Regarding the indirect quantification of ROS, in flasks containing a single plant, there was significantly less electrolyte leakage when infected with *S. sclerotiorum* in the presence of *Trichoderma* (1 P+Th+Ss: 3.312 ± 0.085) compared to plants in its absence (1 P+Ss: 5.489 ± 0.924) (Fig. 3b). In flasks with two plants, there were no significant differences between plants with (3.998 ± 0.09) and without *Trichoderma* (4.956 ± 1.662), when the neighboring plant was not pre-infected 48 h earlier (2 P+Th+Ss-o and 2 P+Ss-o, respectively). Nevertheless, when in flasks with two plants the neighboring plant had been pre-infected with the pathogen 48 h earlier, its neighboring plant showed significantly less electrolyte leakage in the presence of *Trichoderma* (2 P+Th+Ss-w: 0.479 ± 0.161) than in its absence (2 P+Ss-w: 4.938 ± 0.657) (Fig. 3b).

3.2. *Trichoderma*-roots colonization

In single-plant systems (1 P), foliar infection with *S. sclerotiorum* (+Ss) did not significantly increase root colonization by *T. hamatum* (1.198 ± 0.347) (Fig. 4). In flasks with two plants (2 P), colonization by *T. hamatum* was significantly lower (0.415 ± 0.041) than in those with a single plant. When one of the plants in these flasks was infected foliarly with *S. sclerotiorum*, no significant differences in root colonization *by T. hamatum* were reported between that plant (2 P+Th+Ss-o: 2003 ± 0.762) and its neighbor (2 P+Th+Ss-o-np: 1052 ± 0.589). However, in this uninfected neighboring plant (2 P+Th+Ss-o-np), root

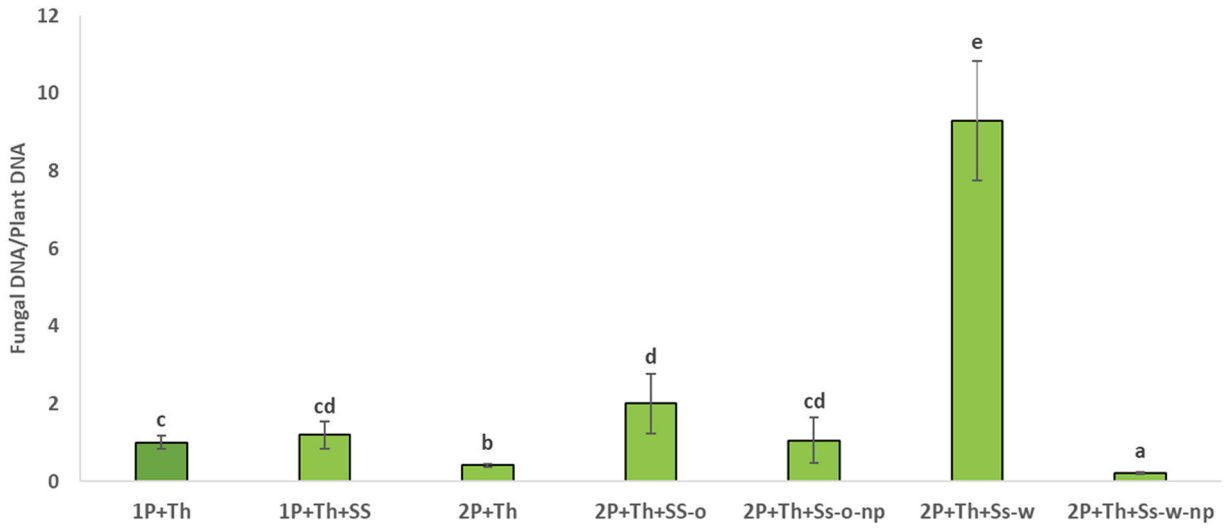

Fig. 4. Measurements of broccoli-root colonization by *T. hamatum* (+Th) in one plant (1 P) or two neighboring plants (2 P), Ss-infected (+Ss) (b). When the neighboring plant was infected 48 h before, the colonization in the neighboring plant (np) was also quantified, and when only the neighboring plant was infected, the colonization was analyzed in the non-infected plant. To quantify broccoli-root colonization, the DNA of the fungus was quantified by qPCR from radicular samples using the *Actin* genes from both the plants and the fungus. Fungal DNA/plant DNA ratio was normalized to 1 in the case of 1 P and was calculated based on this data for the rest of the lines. Data are the mean of 12 plant-roots in 4 pools with the corresponding standard deviation. One-way analysis of variance (ANOVA) was performed, followed by the Tukey's test. Different letters represent significant differences ($P < 0.05$).

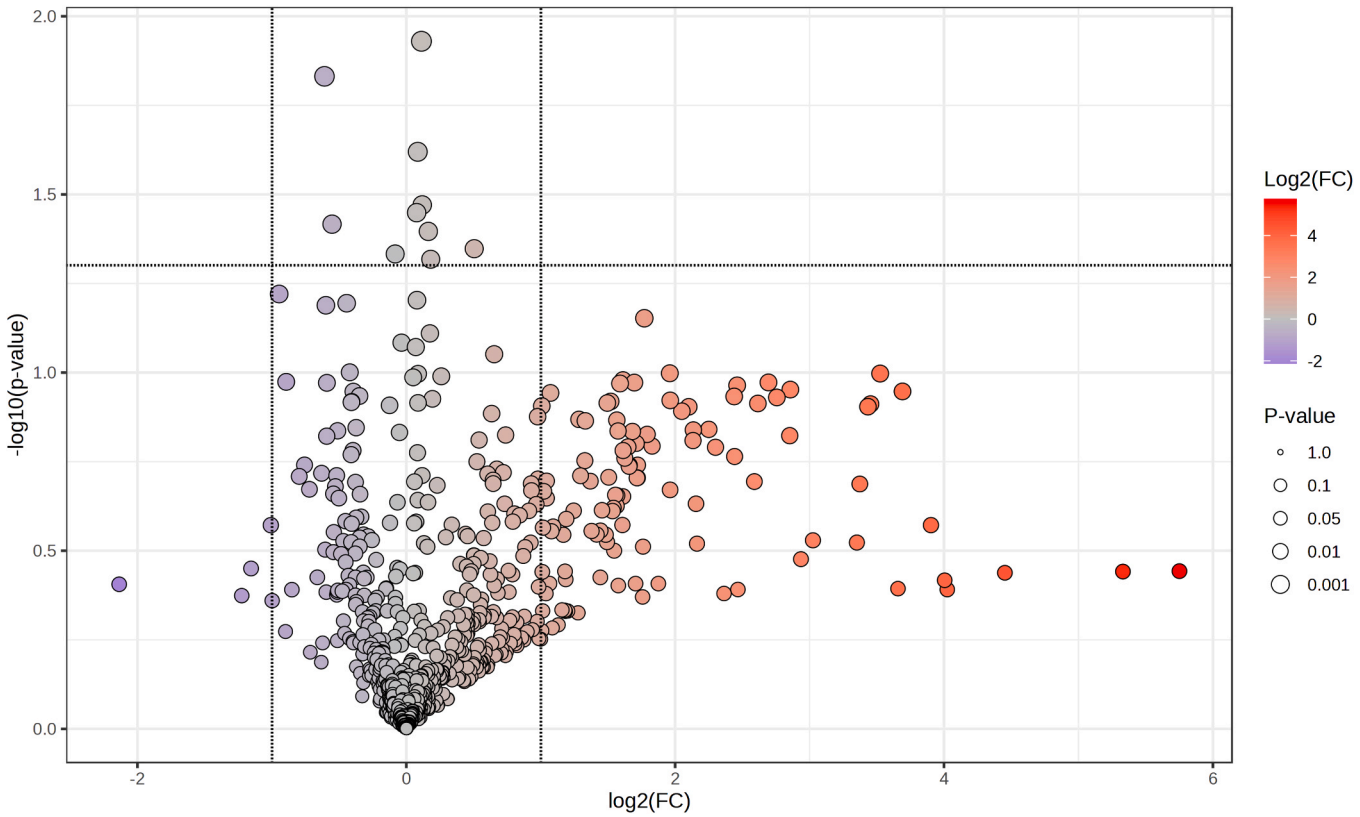

Fig. 5. Volcano plot representing the detected features in the non-targeted metabolomic analysis in *T. hamatum* mycelium. The y-axis represents the negative decade logarithm of the significance value (FDR), and the x-axis represents the log2 of fold change (among all the different conditions studied where *T. hamatum* was inoculated). Levels of features with a $-\log10(p) \leq 1.3$ and a $|\log2(FC)| \geq 1$ are considered to be differentially accumulated. Significantly up-regulated features are represented by red circles and down-regulated features are represented by blue circles. None of the metabolites were significant with these conditions (upper-right corner).

colonization was significantly higher than in the flasks with a single plant (Fig. 4). When the neighboring plant had been pre-infected with the pathogen 48 h before the other, a significant decrease in root colonization levels by *T. hamatum* (0.202 ± 0.025) was quantified in the pre-infected neighboring plant (2 P+Th+Ss-w-np), compared to all other plants and treatments. In contrast, in the other plant in the system

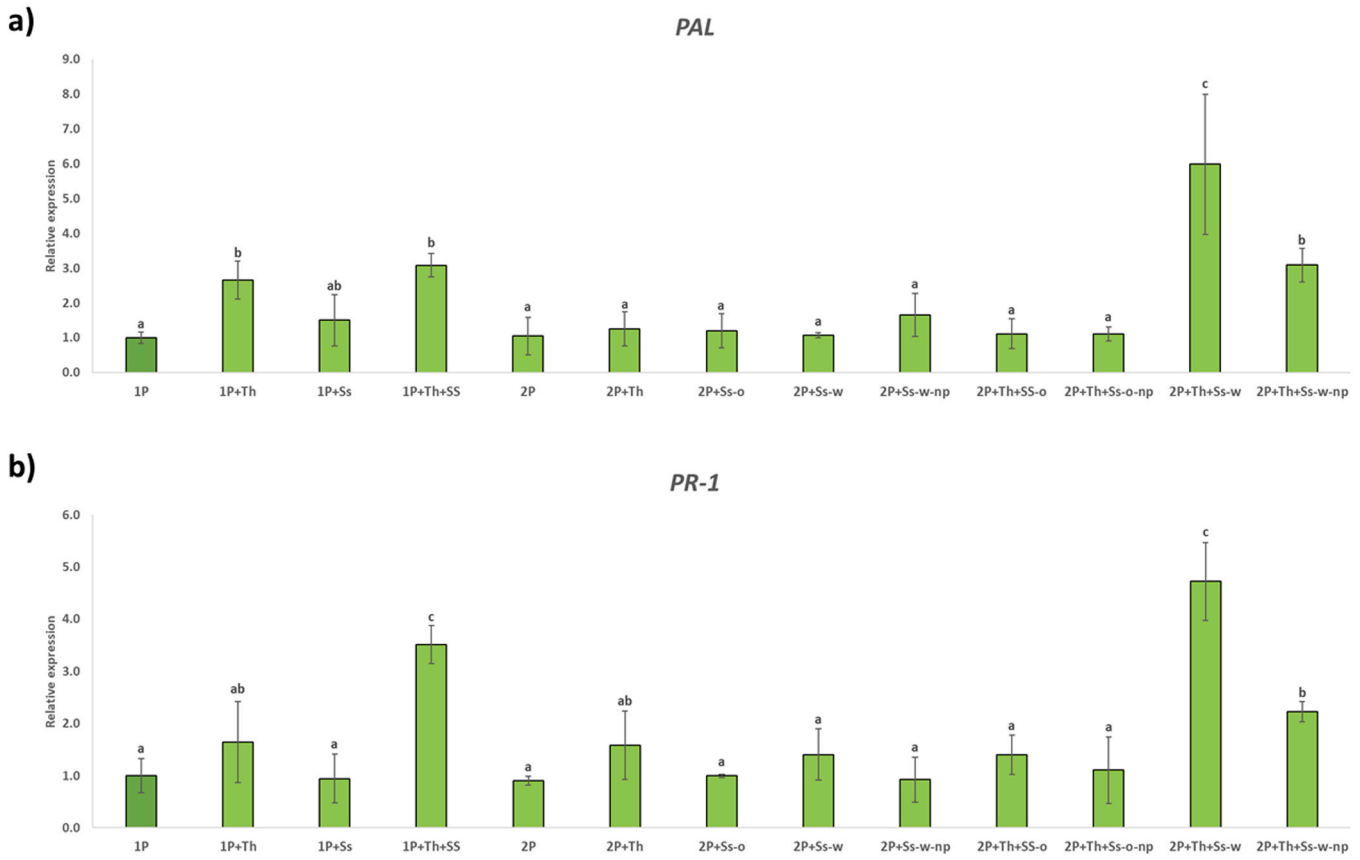

Fig. 6. Quantitative reverse transcription polymerase chain reaction (RT-qPCR) analysis of the expression of some defense SA-related genes in broccoli roots foliar-infected with *S. sclerotiorum* (+Ss) and root inoculated with *T. hamatum* (+Th). When the neighboring plant was infected 48 h before (w), and not infected (o), the gene expression levels in the neighboring plant (np) was also quantified. Genes of the *phenylalanine ammonia lyase* (*PAL*) (a) and *pathogenesis-related 1* (*PR-1*) (b). Values correspond to relative measurements against single plants without *Trichoderma*-roots inoculation (1 P) ($2^{-\Delta\Delta Ct} = 1$). The broccoli *Actin* gene was used as an internal reference gene. Data are the mean of 4 pools of 3 plants each with the corresponding standard deviation. One-way analysis of variance (ANOVA) was performed, followed by the Tukey's test. Different letters represent significant differences ($P < 0.05$).

(2 P+Th+Ss-w), which was infected foliar with *S. sclerotiorum* 48 h after its neighboring plant, a significant increase in root colonization (9.294 ± 1.537) was reported, compared to the rest of the plants and treatments (Fig. 4).

3.3. Metabolomics of T. hamatum mycelium

The features obtained in the different mycelia were analyzed using Volcano Plot at an FDR significance of ≤ 0.05. No significantly differentially present metabolites were reported between the *T. hamatum* mycelia under the different conditions of the study. Nor were any reported when the neighboring plant was previously infected with *S. sclerotiorum* 48 h before infecting the other plant (treatment 2 P+Th+Ss-w) (Fig. 5).

3.4. Defense-genes expression in roots and leaves

The expression of genes related to defense pathways (SA and JA) was analyzed in both the roots and aerial parts of broccoli plants. At the root level, inoculation of a single plant (1 P) with *T. hamatum* (1 P+Th) significantly increased the expression of SA-related genes (Fig. 6) and reduced the expression of JA-related genes (Fig. 7). Similar levels of gene expression were quantified when the plant was colonized at the root by *T. hamatum* and infected at the leaf by *S. slcerotiorum* (1 P+Th+Ss) (Figs. 6 and 7). However, leaf infection without root application of *T. hamatum* (1 P+Ss) did not significantly alter gene expression levels compared to the control (1 P) (Figs. 6 and 7). In systems with two neighboring plants in the same flask (2 P), no significant differences in the expression of the analyzed genes were reported compared to 1 P when there were two plants (2 P), when they were inoculated root-wise with *T. hamatum* (2 P+Th), when either of the two plants was infected foliar-wise with *S. sclerotiorum* (2 P+Ss-o, 2 P+Ss-w and 2 P+Ss-w-np), or when they were inoculated root-wise with *T. hamatum* and the neighboring plant was not previously infected foliar-wise with the pathogen (2 P+Th+Ss-o and 2 P+Th+Ss-o-np) (Figs. 6 and 7). However, when the plants were root colonized by *T. hamatum* and the neighboring plant was infected 48 h earlier than the other plant, in the neighboring plant, a significant increase in the expression of SA-related genes (Fig. 6) and a significant reduction in JA-related genes (Fig. 7), similar to those reported under conditions 1 P+Th and 1 P+Th+Ss. In the plant infected foliarly 48 h after its neighbor (2 P+Th+Ss-w), an even greater significant increase in the expression of SA-related genes (Fig. 6) was quantified, along with a significant reduction in the expression of JA-related genes (Fig. 7), compared to all other conditions.

The gene expression of these defense-related genes in the aerial parts of broccoli plants was also analyzed. In single-plant systems, root inoculation with *T. hamatum* (1 P+Th) caused a significant increase in the expression of SA- and JA-related genes (Figs. 8 and 9). This significant increase in the gene expression of JA-related genes was also reported in single plants infected foliarly with *S. slcerotiorum* (1 P+Ss) (Fig. 9). However, in these plants, there was a significant decrease in the expression of SA-related genes compared to the uninfected control (1 P) (Fig. 8). Plants in single-plant systems that were root-inoculated with

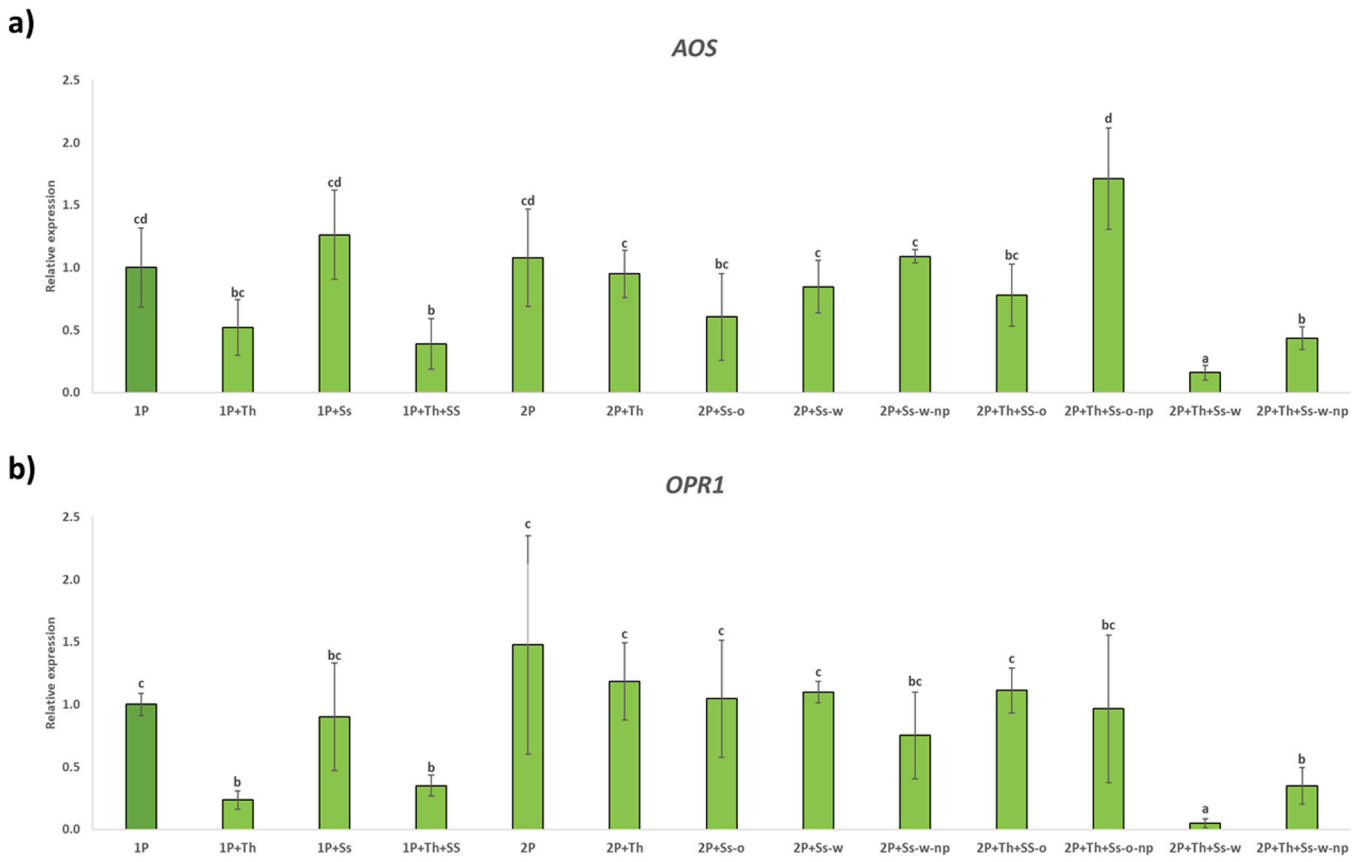

Fig. 7. Quantitative reverse transcription polymerase chain reaction (RT-qPCR) analysis of the expression of some defense JA-related genes in broccoli roots foliar-infected with *S. sclerotiorum* (+Ss) and root inoculated with *T. hamatum* (+Th). When the neighboring plant was infected 48 h before (w), and not infected (o), the gene expression levels in the neighboring plant (np) was also quantified. Genes of the *allene oxide synthase* (*AOS*) (a) and *12-oxophytodienoate reductase 1* (*OPR1*) (b). Values correspond to relative measurements against single plants without *Trichoderma*-roots inoculation (1 P) ($2^{-\Delta\Delta Ct} = 1$). The broccoli *Actin* gene was used as an internal reference gene. Data are the mean of 4 pools of 3 plants each with the corresponding standard deviation. One-way analysis of variance (ANOVA) was performed, followed by the Tukey's test. Different letters represent significant differences ($P < 0.05$).

T. hamatum and foliar-infected with the pathogen reported an even greater increase in the expression of JA-related genes (Fig. 9), with no significant changes in the expression of SA-related genes (Fig. 8). In flasks with two plants (2 P), no significant differences in the expression of these genes were determined compared to single-plant systems (1 P) (Figs. 8 and 9). This same absence of significant differences was also reported when the systems with two plants were root-inoculated with *T. hamatum* (2 P+Th) (Figs. 8 and 9). However, if either of the two plants was foliar infected with *S. sclerotiorum* (2 P+Ss-o, 2+Ss-w and 2 P+Ss-w-np), results similar to those of 1 P+Ss were reported in both plants (Figs. 8 and 9). When these plants were colonized by *T. hamatum* in their roots and one of the plants was infected in its leaves, without prior infection of its neighboring plant, similar levels of expression in its defense genes were reported in the infected plant (2 P+Th+Ss-o) as in the 1 P+Th+Ss condition (Figs. 8 and 9). However, in the neighboring plant (2 P+Th+Ss-o-np), which was not previously infected with the pathogen, no significant changes in gene expression were reported compared to the control plants (1 P and 2 P) (Figs. 8 and 9). When the neighboring plant was pre-infected with S. *sclerotiorum* 48 h before the other, this second plant (2 P+Th+Ss-w) showed a significant decrease in the expression of SA-related genes (Fig. 8) and a significant increase in the expression of JA-related genes (Fig. 9), compared to any other condition studied. In the pre-infected neighboring plant (2 P+Th+Ss-w-np), gene expression levels similar to those in conditions 1 P+Th+Ss and 2 P+Th+Ss-o were reported (Figs. 8 and 9).

3.5. Metabolomics of broccoli tissues

To analyze the metabolic changes caused by the possible communication between plants mediated by *T. hamatum* in broccoli, we performed an untargeted metabolomic analysis. Volcano Plot at an FDR significance of ≤ 0.05 was performed to investigate and visualize the patterns of metabolic changes between the different conditions studied. Roots (Fig. 10) and broccoli aerial parts (Fig. 11) were used to detect metabolites affected by these conditions. The Volcano Plot model was evaluated using cross-validation (R2 and Q2 parameters). The quality assessment (Q2) and R2 statistics provide a qualitative measure of the consistency between the predicted and original data or, in other words, estimate the predictive power of the model. For comparison purposes, features with a VIP score > 2 in the Volcano Plot model were selected and considered the most influential features.

Different conditions were compared in pairs in both the roots and aerial parts of broccoli: 2 P vs. 2 P+Ss-o, 2 P vs. 2 P+Th, and 2 P vs. 2 P+Th+Ss-w. In each tissue type, metabolites differentially present in 2 P+Th+Ss-w compared to the control (2 P) were selected, eliminating common metabolites differentially present in conditions 2 P+Ss-o and 2 P+Th. Based on the above analysis, we selected eight features that were only present in the roots and two in the leaves. We provisionally assigned compound names to three of the eight selected in roots and to the two metabolites selected in leaves (Table 3). In the roots, the metabolites 5-(methylsulfinyl)pentyl nitrile (a sulfoxide), D-1-[(3-carboxypropyl)amino]-1-deoxyfructose (a carboxylic acid derivative), and neoglucobrassicin (a glucosinolate) were identified. Meanwhile,

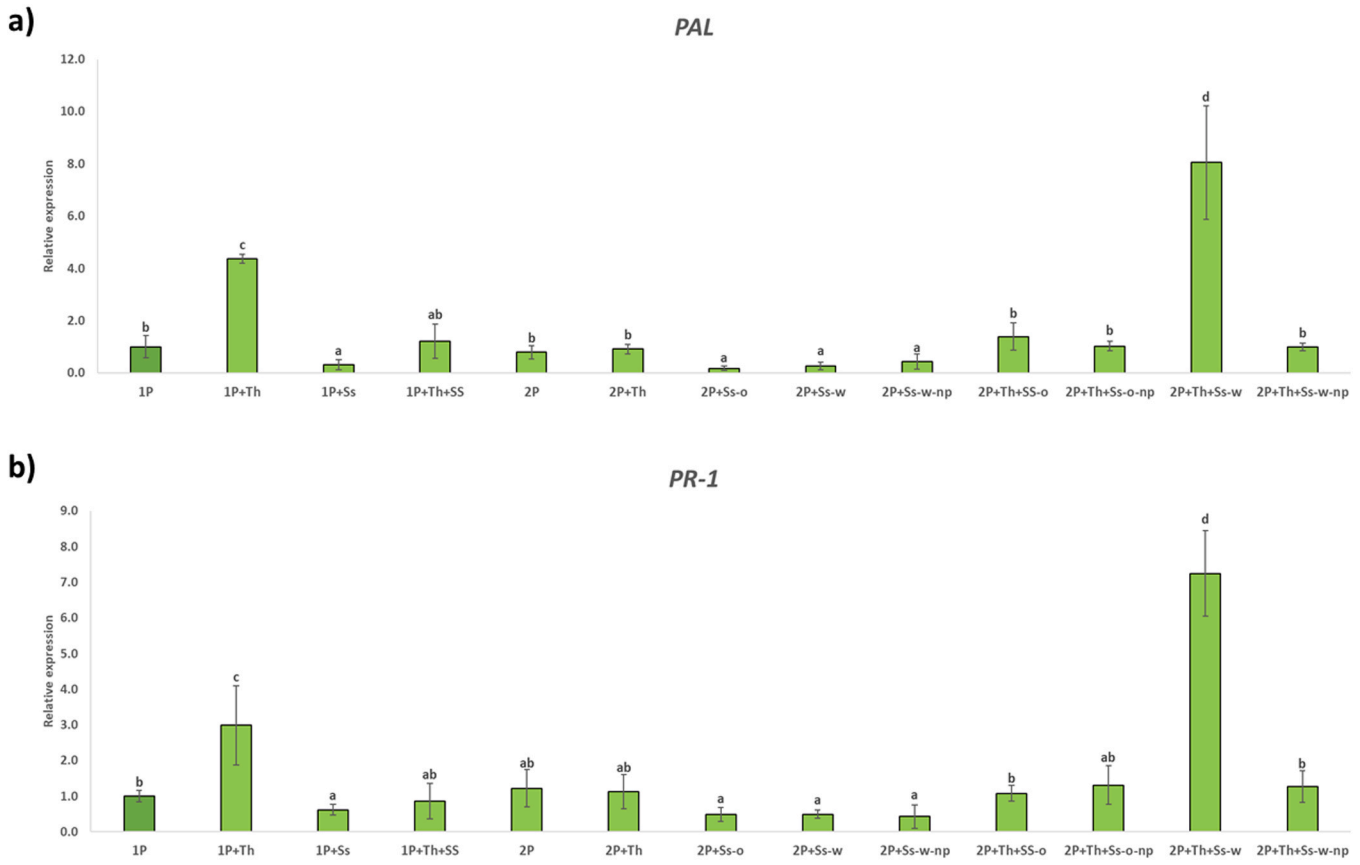

Fig. 8. Quantitative reverse transcription polymerase chain reaction (RT-qPCR) analysis of the expression of some defense SA-related genes in broccoli aerial parts foliar-infected with *S. sclerotiorum* (+Ss) and root inoculated with *T. hamatum* (+Th). When the neighboring plant was infected 48 h before (w), and not infected (o), the gene expression levels in the neighboring plant (np) was also quantified. Genes of the *phenylalanine ammonia lyase* (*PAL*) (a) and *pathogenesis-related 1* (*PR-1*) (b). Values correspond to relative measurements against single plants without *Trichoderma*-roots inoculation (1 P) ($2^{-\Delta\Delta Ct} = 1$). The broccoli *Actin* gene was used as an internal reference gene. Data are the mean of 4 pools of 3 plants each with the corresponding standard deviation. One-way analysis of variance (ANOVA) was performed, followed by the Tukey's test. Different letters represent significant differences ($P < 0.05$).

pantheric acid and oxodocosanoic acid (lipids) were identified in the leaves (Table 3).

4. Discussion

Although communication between plants via hyphal networks has been widely described and studied with mycorrhizal fungi (reviewed by Johnson and Gilbert, 2015; Gilbert and Johnson, 2017; Simard, 2018; Boyno and Demir, 2022), the involvement of other groups of fungi is still largely unknown. To date, only two studies have investigated this type of "wired communication" with endophytic fungi. These previous studies described the ability of *P. indica* (Vahabi et al., 2018) and *T. hamatum* (Poveda et al., 2023a) to induce defenses in neighboring plants, following foliar infection of the other neighboring plant, through the physical connection of their roots by fungal hyphae. Furthermore, in both cases, the plant hormone JA played a key role in the induction of plant defenses by endophytic fungi (Vahabi et al., 2018; Poveda et al., 2023a). However, it is unknown whether this biological phenomenon can be reproduced in crops of agricultural interest or whether metabolic changes in the endophytic fungus are involved in the observed results of plant defense induction, also at the metabolic level. This work aims to delve deeper into this type of communication between plants, attempting to answer these questions, for which it has required the development of a novel plant-fungus cultivation system in an axenic system.

In single-plant (1 P) systems, root inoculation with *T. hamatum* reduced leaf lesions caused by the necrotrophic pathogen *S. sclerotiorum*, due to induction of JA-mediated defenses, a fundamental defense pathway against necrotrophic pathogens (Macioszek et al., 2023). The ability of different *Trichoderma* species to induce systemic defenses in different *Brassica* crops through root colonization has been widely addressed in recent years against various necrotrophic pathogens, such as *S. sclerotiorum*, *A. brassicae* or *Leptosphaeria maculans* (reviewed by Sánchez-Gómez et al., 2025). Although our work represents the first description of the induction of systemic defenses against *S. sclerotiorum* in broccoli plants by *Trichoderma* root colonization, this mechanism of action has been reported in other plant species. In brinjal, *Trichoderma harzianum* and *T. asperellum* induced systemic metabolic and enzymatic plant defenses against the necrotrophic pathogen (Singh et al., 2021). Specifically, with *T. hamatum*, root colonization of *A. thaliana* roots leads to the induction of effective systemic defenses in the lower incidence of *S. sclerotiorum* (Poveda et al., 2023a). However, we have been able to report that foliar infection with the pathogen does not lead to an increase in root colonization of broccoli plants by *T. hamatum*. Therefore, the plant would benefit from pre-existing fungal root colonization, without actively facilitating higher levels of colonization. Although numerous previous studies have described how plants attacked by leaf pathogens actively induce the recruitment and root colonization of microorganisms that induce systemic defenses (Wen et al., 2021).

In two-plant systems (2 P) without prior infection of the neighboring plant (-o), however, root inoculation of broccoli plants with *T. hamatum* did not result in a reduction in foliar infection by the necrotrophic pathogen. This result could be related to the lower root colonization by *T. hamatum* quantified in these plants. It has previously been described

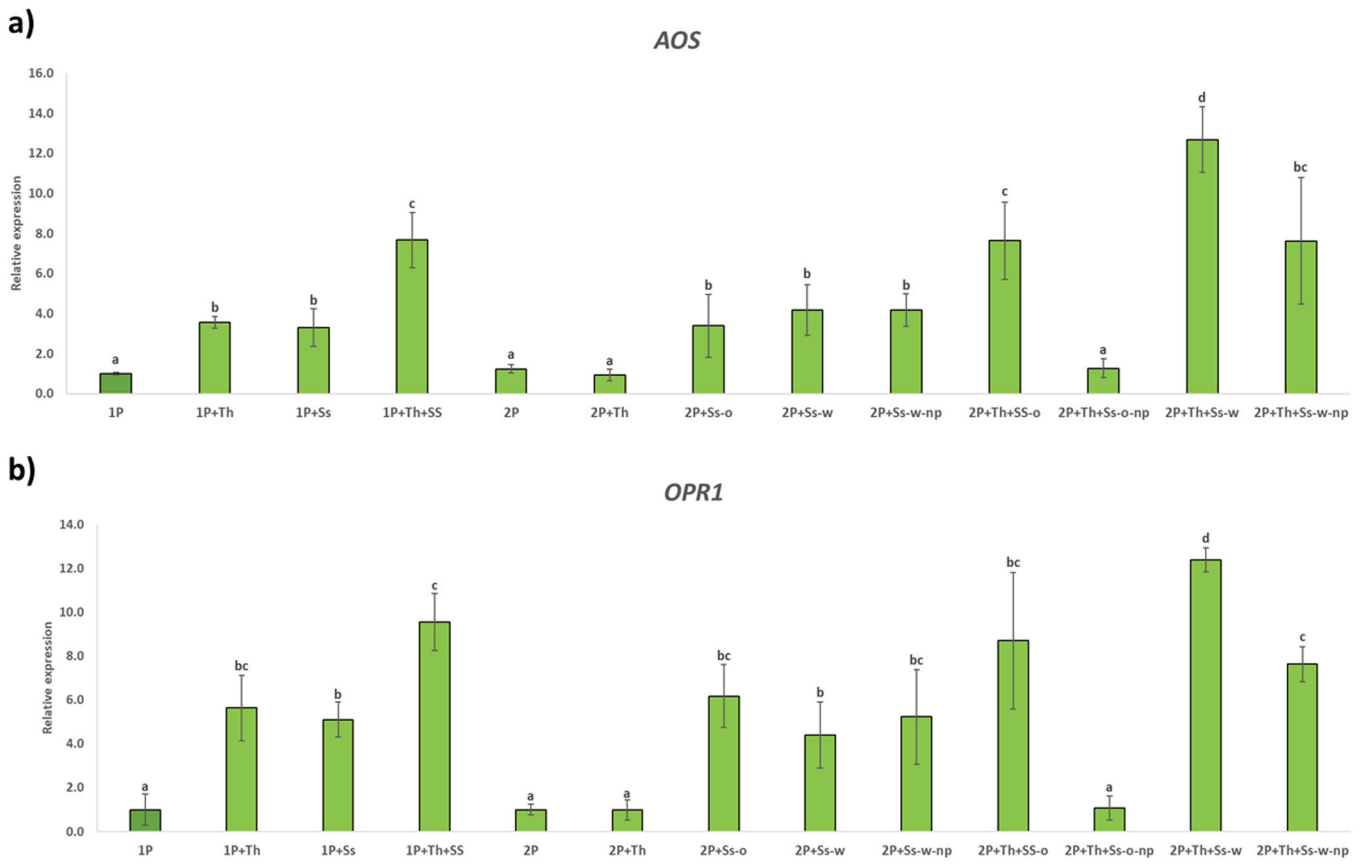

Fig. 9. Quantitative reverse transcription polymerase chain reaction (RT-qPCR) analysis of the expression of some defense JA-related genes in broccoli aerial parts foliar-infected with *S. sclerotiorum* (+Ss) and root inoculated with *T. hamatum* (+Th). When the neighboring plant was infected 48 h before (w), and not infected (o), the gene expression levels in the neighboring plant (np) was also quantified. Genes of the *allene oxide synthase* (*AOS*) (a) and 1*2-oxophytodienoate reductase 1* (*OPR1*) (b). Values correspond to relative measurements against single plants without *Trichoderma*-roots inoculation (1 P) ($2^{-\Delta\Delta Ct} = 1$). The broccoli *Actin* gene was used as an internal reference gene. Data are the mean of 4 pools of 3 plants each with the corresponding standard deviation. One-way analysis of variance (ANOVA) was performed, followed by the Tukey's test. Different letters represent significant differences ($P < 0.05$).

that greater root colonization by *Trichoderma* leads to an increase in the systemic defenses of the host plant. This was observed in chickpea plants colonized by *T. harzianum*, which induced higher levels of ET-mediated defenses against the pathogenic fungus *Ascochyta rabiei* (Morcuende et al., 2024). Or in *A. thaliana* plants with *T. harzianum*, *T. parareesei* (Poveda, 2021) and *T. hamatum* (Poveda et al., 2023a), against the necrotrophs *Botrytis cinerea* and *S. sclerotiorum*, through the induction of JA-mediated defenses.

The lower root colonization by *T. hamatum* reported in our broccoli plants when there were two neighboring plants was also previously described in *A. thaliana* plants in soil (Poveda et al., 2023a). However, this is contrary to what has been previously described with mycorrhizal fungi, whose root colonization increases significantly as the number of neighboring plants increases (Šmilauer et al., 2020).

In the absence of *T. hamatum* in the system, pre-infection of the neighboring plant with *S. sclerotiorum* 48 h before the other plant did not produce significant differences in the lesions caused by the pathogen. Although very different mechanisms of interplant communication that could occur in our system have been described, the absence of lower infection in the second plants is indicative of an absence or low effectiveness of the signal sent by the plant previously infected by the pathogen. The most studied inter-plant communication mechanism that could easily occur in our system is the emission of defense-inducing VOCs, such as methyl salicylate (MeSA) or methyl jasmonate (MeJA) (Bergman et al., 2025), since it is an axenic and closed cultivation system.

However, when in systems with two plants, one of which had been pre-infected with *S. sclerotiorum* 48 h before its neighbor and both were colonized at the roots with *T. hamatum*, the lesions caused by the pathogen were almost non-existent. In these more resistant plants, higher levels of JA-related gene expression were quantified than in any other plant. Therefore, *T. hamatum* is capable of communicating between two neighboring plants, "warning" one plant of the foliar infection of its neighbor so that it can induce its JA-mediated defenses, specific against necrotrophic pathogens (Macioszek et al., 2023).

One of the questions to be resolved in our work is to determine how *T. hamatum* sends information between plants. We analyzed the interplant mycelium in all the systems studied to determine whether any differentially accumulated metabolites could be involved. However, we did not identify any differentially present metabolites in the mycelium of any of the systems. The mechanism of interplant communication does not appear to be through metabolites mobilized/accumulated in the tissues of *T. hamatum*.

On the other hand, we also studied the levels of root colonization by *T. hamatum* in all plants. In the neighboring plant pre-infected foliarly 48 h earlier, we reported lower levels of root colonization. Foliar pre-infection caused a significant increase in the expression of JA-related genes in the aerial part of these plants, which led to an antagonistic increase in the expression of SA-related genes at the root level, an antagonism of hormonal responses that has been widely described previously (Hou and Tsuda, 2022). This increase in SA-mediated root defenses in the roots is directly related to the lower colonization reported with *T. hamatum*, as it is the key plant hormone in controlling plant colonization by *Trichoderma*. In the absence of SA, the plant cannot limit

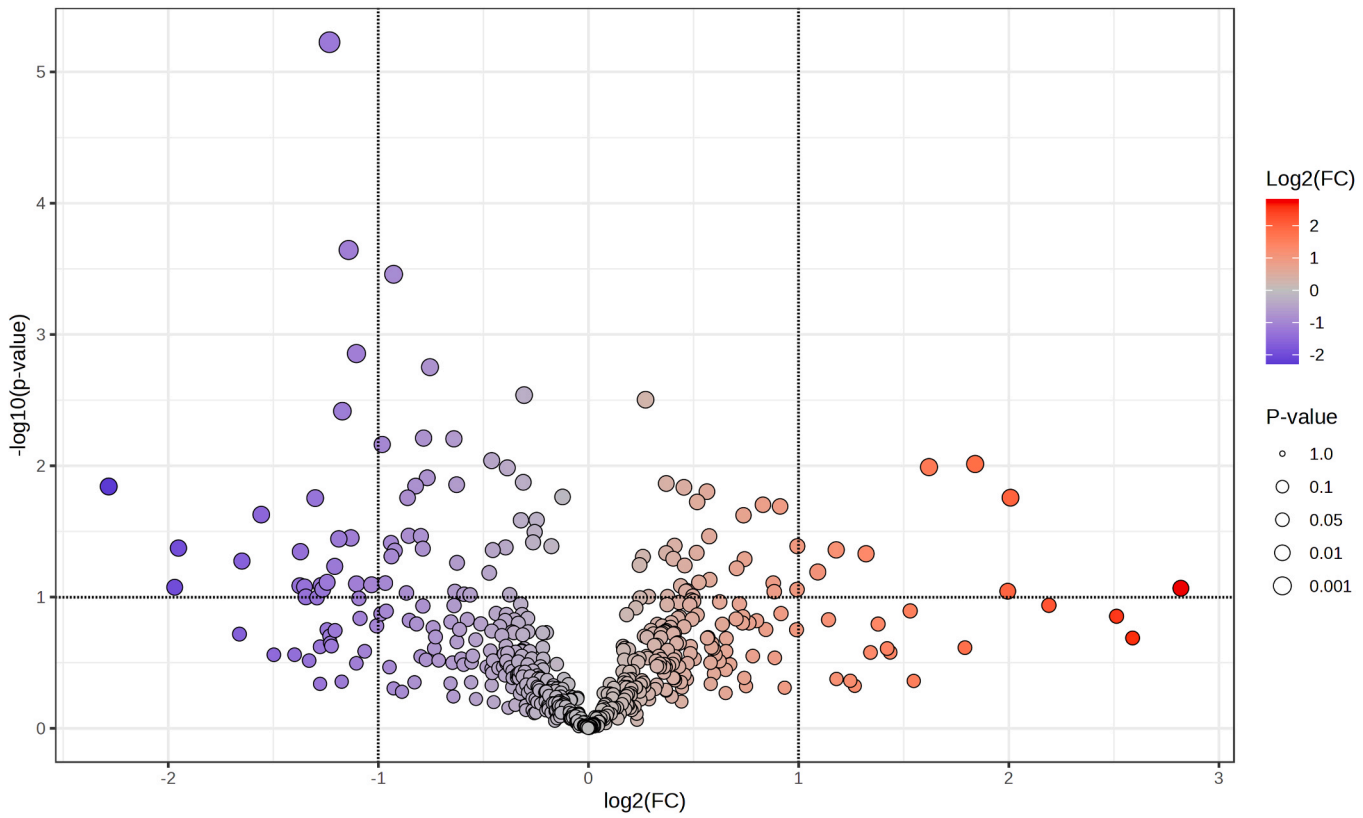

Fig. 10. Volcano plot representing the detected features in the non-targeted metabolomic analysis in broccoli roots. The two pairs of conditions used in the analysis weretwo neighboring plants (2 P) vs. two neighboring plants with *T. hamatum* inoculation and foliar infected with *S. sclerotiorum*, with neighbor plant infected 48 h before (2 P+Th+Ss-w). Up-regulated metabolites (red circles) with an FDR lower than 0.05 were selected (upper-right corner).

Trichoderma colonization and the fungus reaches the vascular bundles, behaving as a systemic pathogen (Alonso-Ramírez et al., 2014; Poveda et al., 2023b).

In the case of the neighboring plant infected 48 h after its companion, we reported a large increase in root colonization by *T. hamatum*, the expression of genes related to root SA and related to JA in the aerial part. Therefore, the inability of *T. hamatum* to colonize the roots of the first plant infected foliarly with *S. sclerotiorum* led to an increase in root colonization of the neighboring plant. To defend itself against such massive root colonization, the plant activated its local SA-mediated defenses, a specific response to control colonization by *Trichoderma*. This led to a large antagonistic increase in the expression of JA-related genes in the leaves, which led to less infection by *S. sclerotiorum*.

In addition to the expression of defense-related genes, we studied the differentially present metabolites in plant tissues. Plant metabolites previously associated with plant defenses were found in the roots of plants that had been "warned" by *T. hamatum* of leaf infection in their neighboring plant. The metabolite D-1-[(3-carboxypropyl)amino]-1-deoxyfructose is related to plant antioxidant responses to different stresses (Dave et al., 2018; Kamaruddin et al., 2021), although this metabolite has not been linked to SA-mediated signaling.

The GSL neoglucobrassicin is a metabolite widely associated with specific plant defenses against different fungal pathogens of *Brassica* crops (Rubel et al., 2020; Zamani-Noor et al., 2021). Furthermore, the synthesis and accumulation of this metabolite is induced by SA-mediated defense signaling (Yi et al., 2016). Therefore, the local SA-mediated defense in these plants, to prevent uncontrolled colonization by *T. hamatum*, is carried out, in addition to other mechanisms, through the accumulation of neoglucobrassicin. In this regard, it was previously determined that indole GSLs (such as neoglucobrassicin) are specifically involved in controlling *Trichoderma* root colonization levels in *A. thaliana* roots (Poveda, 2021).

In addition, significantly higher levels of the GSL hydrolysis product (GHP) 5-(methylufinyl)pentyl nitrile were found in these roots. The hydrolysis of GSLs by myrosinase enzymes causes the formation of antifungal compounds called isothiocyanates. However, the binding of these enzymes to nitrile-specifier and epithiospecifier proteins can modify this hydrolysis towards less toxic compounds, such as nitriles and epithionitriles (Abdel-Massih et al., 2023). It has been described how *Trichoderma* requires this type of protein to modify the hydrolysis of GSLs in Brassicaceae plants and thus be able to colonize their roots (Poveda et al., 2019; Nicolás et al., 2024). Therefore, the higher amount of 5-(methylufinyl)pentyl nitrile in the roots of broccoli massively colonized by *T. hamatum* could be the result of the action of fungal nitrile-specifier proteins necessary for the success of its root colonization.

On the other hand, two metabolites were identified as being differentially present in large quantities in the broccoli tissues most resistant to the pathogen, having received communication between plants mediated by *T. hamatum* from the neighboring preinfected plant. These metabolites were the lipids pantheric acid and oxodocosanoic acid, both previously described as being involved in JA-mediated plant defense responses (Kallenbach et al., 2011; Wang et al., 2025). Therefore, the induction of defenses in broccoli by *T. hamatum* mediated by JA could involve an increase in the foliar accumulation of pantheric acid and oxodocosanoic acid, which could increase resistance to *S. sclerotionum*.

Because *in vitro* systems often amplify growth-defense trade-offs, it is possible that defense activation in broccoli occurred under a different metabolic cost structure than in soil-grown conditions (He et al., 2022). Although our results show consistent hormonal and metabolomic patterns independent of biomass, this factor should be considered when extrapolating the magnitude of the response to field environments.

Therefore, it is proposed that the mechanism by which *T. hamatum* communicates with neighboring plants is through its root colonization

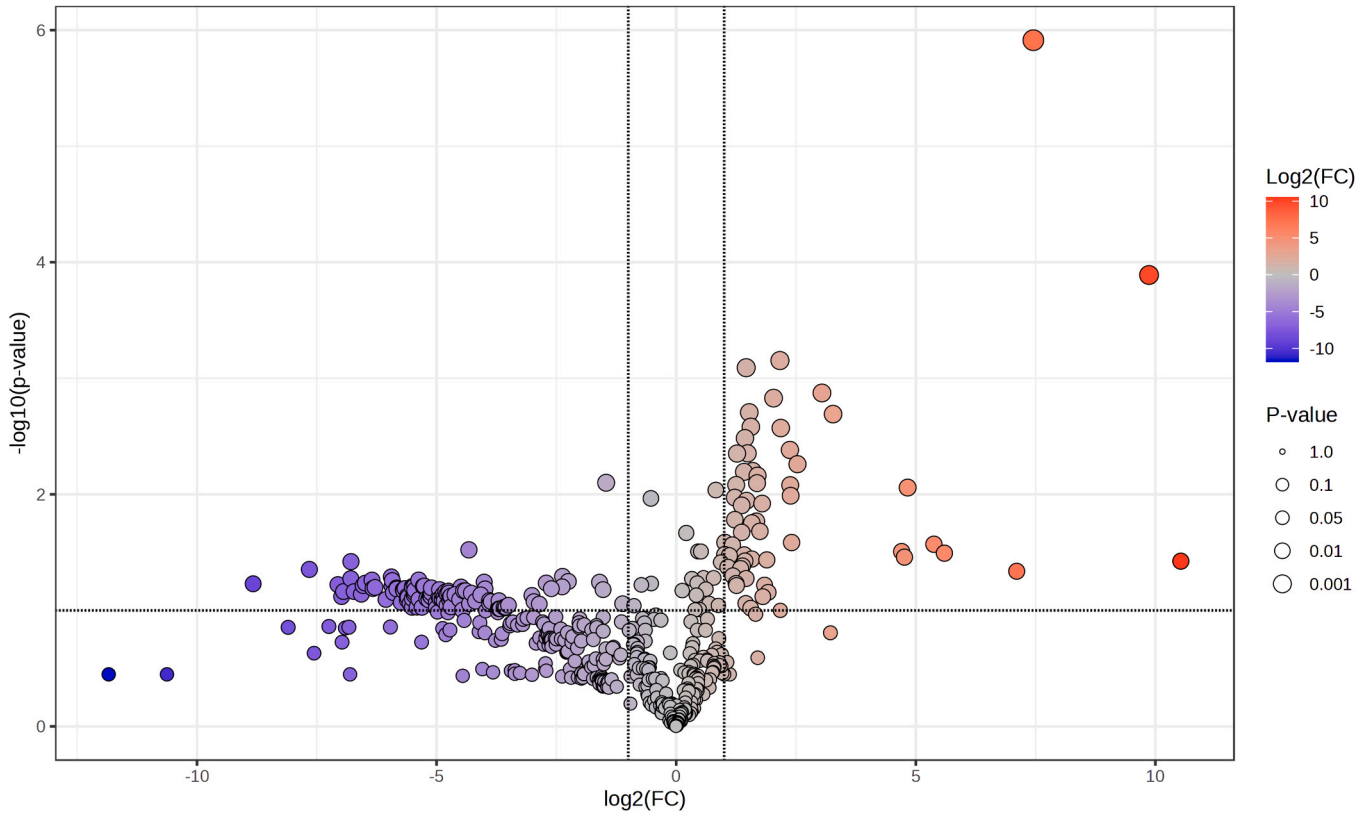

Fig. 11. Volcano plot representing the detected features in the non-targeted metabolomic analysis in broccoli aerial parts. The two pairs of conditions used in the analysis weretwo neighboring plants (2 P) vs. two neighboring plants with *T. hamatum* inoculation and foliar infected with *S. sclerotiorum*, with neighbor plant infected 48 h before (2 P+Th+Ss-w). Up-regulated metabolites (red circles) with an FDR lower than 0.05 were selected (upper-right corner).

Table 3
Tentative identification of metabolites selected after a Volcano Plot analysis.

Plant Matherial	Neutral Mass (Da)	RT (s)	mz	Ionization	Formula	Fragments	Tentative Identification	CLASS
Roots	145.05597	188.02	146.0632	+	C6H11NOS	55.289, 64.97	5-(Methylsufinyl)pentyl nitrile	Sulfoxides
	236.06215	828.29	237.0694	+	C11H12N2O2S	57.07, 103.053, 132.048, 162.037	-	-
	265.11636	60.51	266.1237	+	C10H19NO7	230.104, 128.071, 98.029, 87.341	D-1-[(3-Carboxypropyl) amino]-1-deoxyfructose	Carboxylic acids and drivatives
	324.21950	1180.11	325.2268	+	C21H28N2O	223.166, 86.097, 84.081, 71.085	-	-
	466.34129	1711.89	467.3486	+	C26H46N2O5	-	-	-
	959.54956	1306.69	960.5568	+	C46H83N5O12P2	-	-	-
	478.07151	840.31	477.0642	-	C17H22N2O10S2	96.961, 79.958	Neoglucobrassicin	Glucosinolates
	538.17489	61.56	537.1676	-	C24H30N2O12	195.053, 96.97, 61.989	-	Glycosylamines
Aerial parts	352.29609	1731.18	375.2851	+	C22H40O3	250.171, 69.072, 89.059, 195.127	Pantheric acid	Lipids and lipid like molecules
	354.31311	1708.14	353.3058	-	C22H42O3	335.298, 283.27	Oxodocosanoic acid	Lipids and lipid like molecules

levels, which lead to defensive changes at the local (root) and systemic (leaf) levels. Although these results are consistent with those reported in *A. thaliana* plants and *T. hamatum* (Poveda et al., 2023a), they differ from those described with *P. indica* (Vahabi et al., 2018). In this second study, the levels of root colonization by the fungus were not studied, and it was assumed that the fungus perceived local root changes related to JA, which are transmitted by the mycelium to the neighboring plant. Unlike our previous findings in *A. thaliana* (Poveda et al., 2023a), where defense induction was described but the mechanistic basis remained unresolved, the present study demonstrates that the communication signal in broccoli is not metabolic but instead relies on differential root colonization levels by *T. hamatum*.

Limitations of the *in vitro* closed system used in this study should be acknowledged. Because the flask environment is sealed, multiple stimuli may accumulate simultaneously, including plant- and fungus-derived VOCs, pathogen-induced VOCs and stress-related metabolic changes (Sharifi et al., 2022). Growth-defense trade-offs may also be amplified in axenic systems, as recently demonstrated in controlled environments (He et al., 2022). Moreover, *T. hamatum* is known to produce bioactive volatile compounds such as 6-pentyl-2H-pyran-2-one (6-PP), which exhibit antimicrobial activity (Hu et al., 2024) and can modulate plant growth and defense responses (Garnica-Vergara et al., 2016). The antimicrobial activity of the *T. hamatum* VOCs may have contributed to reduced pathogen growth, although our current setup does not separate

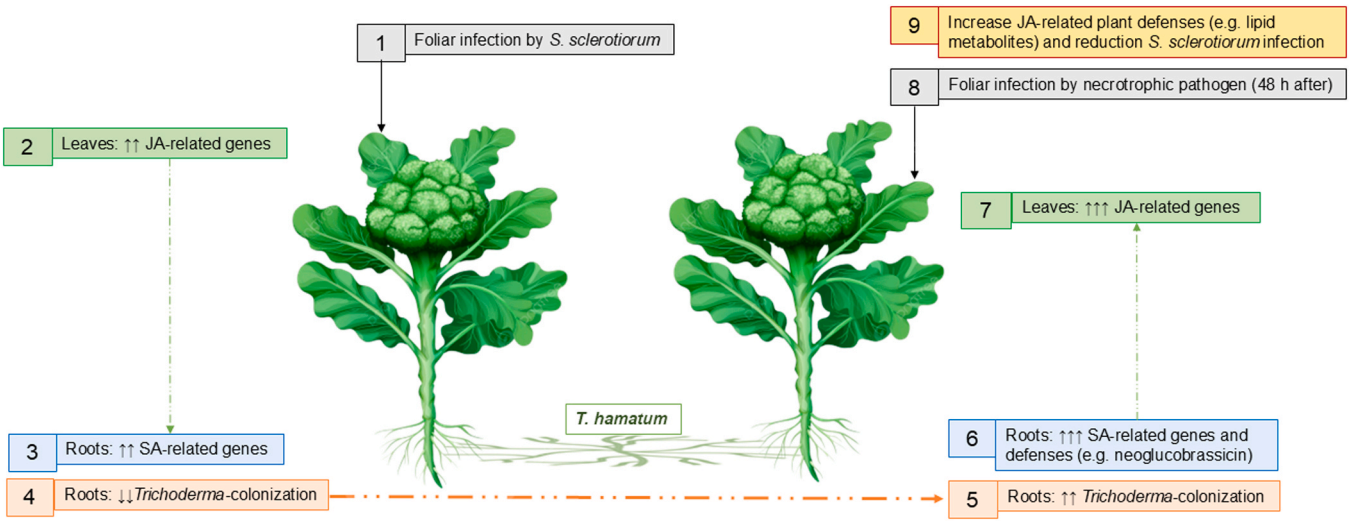

Fig. 12. Infographic summary the possible mechanism involved in the ability of *T. hamatum* to act as inter-plant communicator in foliar infections by *S. sclerotiorum* in broccoli plants. In the initially infected plant, a local foliar defense response mediated by JA is triggered, which antagonistically enhances salicylic acid SA-dependent defenses in the roots. These root defenses restrict colonization by *T. hamatum*, leading to extensive root colonization of a neighboring plant. To prevent systemic infection, this second plant strongly activates local SA-mediated root defenses, including the accumulation of neoglucobrassicin. This root-level SA response, in turn, induces an antagonistic activation of JA-mediated defenses in the leaves, such as the production of lipid metabolites. As a result, when the leaves are later challenged by a necrotrophic pathogen, the pre-activated defenses reduce or prevent foliar infection.

this effect from root colonization dependent mechanisms. Likewise, *S. sclerotiorum* and infected plant tissues emit VOCs that plants can perceive as defense-inducing cues (Moreira et al., 2021). Although *S. sclerotiorum* derived VOCs may contribute to inter-plant warning signals, our controls without *T. hamatum* did not show enhanced resistance, suggesting that pathogen VOCs alone were insufficient to trigger the strong JA-mediated response observed. In addition, stress-induced changes in root exudation are known to influence *Trichoderma* root colonization dynamics (Lombardi et al., 2018). Stress induced changes in root exudation may modulate *T. hamatum* colonization, as previously described in other plant-microbe systems. This factor may contribute to the asymmetric colonization reported between neighboring plants. Although our metabolomic and colonization data indicate that the phenomenon observed here is primarily associated with differential root colonization rather than fungal metabolic reprogramming, we cannot rule out contributions from VOCs or root-exudate-mediated signaling. Future work using ventilated, VOC-isolated or split-root systems will be required to disentangle these factors.

In conclusion, root colonization of broccoli plants by *T. hamatum* induces systemic resistance against foliar infection by the necrotrophic pathogen *S. sclerotiorum*. When two plants are neighbors, *T. hamatum* acts as an effective communicator between plants through root system colonization. Fig. 12 shows the proposed model of the role of *T. hamatum* in this communication between broccoli plants against foliar infection by *S. sclerotiorum*. In the first infected plant, a local foliar defense response against the pathogen occurs, mediated by JA, which causes an antagonistic increase in SA-mediated defenses in the roots. These local defenses at the root level limit root colonization by *T. hamatum*, causing massive root colonization of the other neighboring plant. This second plant must limit the massive root colonization of *T. hamatum* to prevent it from becoming a systemic pathogen, so it massively activates its local SA-mediated defenses, such as the accumulation of the GSL neoglucobrassicin. This local root activation of SA-mediated defenses causes a massive antagonistic induction of JA-mediated defenses at the foliar level, such as the accumulation of lipid metabolites. When the leaf is attacked by the necrotrophic pathogen, the previously activated defenses reduce or prevent foliar infection.

CRediT authorship contribution statement

Jorge Poveda: Writing – review & editing, Writing – original draft, Visualization, Validation, Supervision, Methodology, Investigation, Formal analysis, Conceptualization. **Pablo Velasco:** Writing – review & editing, Visualization, Supervision, Investigation, Formal analysis, Conceptualization. **Shiying Qu:** Investigation.

Declaration of Competing Interest

The authors declare that they have no known competing financial interests or personal relationships that could have appeared to influence the work reported in this paper.

Data Availability

Data will be made available on request.

References

Abdel-Massih, R.M., Debs, E., Othman, L., Attieh, J., Cabrerizo, F.M., 2023. Glucosinolates, a natural chemical arsenal: more to tell than the myrosinase story. Front. Microbiol 14, 1130208. https://doi.org/10.3389/fmicb.2023.1130208.

Afzal, I., Sabir, A., Sikandar, S., 2021. *Trichoderma*: Biodiversity, abundances, and biotechnological applications. In: Yadav, A.N. (Ed.), Recent Trends in Mycological Research: Volume 1: Agricultural and Medical Perspective. Springer, Berlin, Germany, pp. 293–315.

Agrawal, A.A., 2000. Communication between plants: this time it's real. Trends Ecol. Evol. 15 (11), 446. https://doi.org/10.1016/S0169-5347(00)01987-.

Alonso-Ramírez, A., Poveda, J., Martín, I., Hermosa, R., Monte, E., Nicolás, C., 2014. Salicylic acid prevents *Trichoderma harzianum* from entering the vascular system of roots. Mol. Plant Pathol. 15, 823–831. https://doi.org/10.1111/mpp.12141.

Baldwin, I.T., Schultz, J.C., 1983. Rapid changes in tree leaf chemistry induced by damage: evidence for communication between plants. Science 221 (4607), 277–279. https://doi.org/10.1126/science.221.4607.277.

Bergman, M.E., Huang, X.Q., Baudino, S., Caissard, J.C., Dudareva, N., 2025. Plant volatile organic compounds: emission and perception in a changing world. Curr. Opin. Plant Biol. 85, 102706. https://doi.org/10.1016/j.pbi.2025.102706.

Boyno, G., Demir, S., 2022. Plant-mycorrhiza communication and mycorrhizae in inter-plant communication. Symbiosis 86, 155–168. https://doi.org/10.1007/s13199-022-00837-0.

Chong, J., Wishart, D.S., Xia, J., 2019. Using MetaboAnalyst 4.0 for comprehensive and integrative metabolomics data analysis. Curr. Protoc. Bioinform. 68, e86. https://doi.org/10.1002/cpbi.86.

Dave, R., Gajera, H., Ukani, P., Shihora, M., Antala, T., Golakiya, B., 2018. Evaluation of antioxidant activity, untargeted metabolite profile and elemental analysis of *Euphorbia hirta* L. Int. J. Chem. Stud. 6, 1986–1998.

dos Santos, L.B.P.R., Oliveira-Santos, N., Fernandes, J.V., Jaimes-Martinez, J.C., De Souza, J.T., Cruz-Magalhães, V., Loguercio, L.L., 2022. Tolerance to and alleviation of abiotic stresses in plants mediated by *Trichoderma* spp. In: Amaresan, N., Sankaranarayanan, A., Dwivedi, M.K., Druzhinina, I.S. (Eds.), Advances in Trichoderma biology for agricultural applications. Springer, Berlin, Germany, pp. 321–359.

Dührkop, K., Fleischauer, M., Ludwig, M., Aksenov, A.A., Melnik, A.V., Meusel, M., et al., 2019. SIRIUS 4: a rapid tool for turning tandem mass spectra into metabolite structure information. Nat. Methods 16, 299–302. https://doi.org/10.1038/s41592-019-0344-8.

Fang, H., Luo, F., Li, P., Zhou, Q., Zhou, X., Wei, B., et al., 2020. Potential of jasmonic acid (JA) in accelerating postharvest yellowing of broccoli by promoting its chlorophyll degradation. Food Chem. 309, 125737. https://doi.org/10.1016/j.foodchem.2019.125737.

Garnica-Vergara, A., Barrera-Ortiz, S., Muñoz-Parra, E., Raya-González, J., Méndez-Bravo, A., Macías-Rodríguez, L., et al., 2016. The volatile 6-pentyl-2H-pyran-2-one from *Trichoderma atroviride* regulates *Arabidopsis thaliana* root morphogenesis via auxin signaling and ETHYLENE INSENSITIVE 2 functioning. N. Phytol. 209, 1496–1512. https://doi.org/10.1111/nph.13725.

Gilbert, L., Johnson, D., 2017. Plant–plant communication through common mycorrhizal networks. Advances in botanical research. Academic Press, pp. 83–97.

Guo, Y., Gong, C., Cao, B., Di, T., Xu, X., Dong, J., et al., 2023. Blue light enhances health-promoting sulforaphane accumulation in broccoli (*Brassica oleracea* var. *italica*) sprouts through inhibiting salicylic acid synthesis. Plants 12, 3151. https://doi.org/10.3390/plants12173151.

Gupta, N., 2020. *Trichoderma* as Biostimulant: Factors responsible for plant growth promotion. In: Manoharachary, C., Singh, H.B., Varma, A. (Eds.), Trichoderma: Agricultural Applications and Beyond. Springer, Berlin, Germany, pp. 287–309.

Guzmán-Guzmán, P., Kumar, A., de Los Santos-Villalobos, S., Parra-Cota, F.I., Orozco-Mosqueda, M.D.C., Fadiji, A.E., et al., 2023. *Trichoderma* species: our best fungal allies in the biocontrol of plant diseases—a review. Plants 12, 432. https://doi.org/10.3390/plants12030432.

Han, F., Liu, Y., Fang, Z., Yang, L., Zhuang, M., Zhang, Y., et al., 2021. Advances in genetics and molecular breeding of broccoli. Horticulturae 7, 280. https://doi.org/10.3390/horticulturae7090280.

He, Z., Webster, S., He, S.Y., 2022. Growth–defense trade-offs in plants. Curr. Biol. 32, 634–639. https://doi.org/10.1016/j.cub.2022.04.070.

Hossain, M.M., Sultana, F., Li, W., Tran, L.S.P., Mostofa, M.G., 2023. *Sclerotinia sclerotiorum* (Lib.) de Bary: Insights into the pathogenomic features of a global pathogen. Cells 12, 1063. https://doi.org/10.3390/cells12071063.

Hou, S., Tsuda, K., 2022. Salicylic acid and jasmonic acid crosstalk in plant immunity. Essays Biochem 66, 647–656. https://doi.org/10.1042/EBC20210090.

Hu, X., Shi, H., Zhang, Z., Bai, C., 2024. Antifungal effects of volatile organic compounds produced by *Trichoderma hamatum* against *Neocosmospora solani*. Lett. Appl. Microbiol 77, ovae063. https://doi.org/10.1093/lambio/ovae063.

Johnson, D., Gilbert, L., 2015. Interplant signalling through hyphal networks. N. Phytol. 205, 1448–1453. https://doi.org/10.1111/nph.13115.

Kallenbach, M., Gilardoni, P.A., Allmann, S., Baldwin, I.T., Bonaventure, G., 2011. C12 derivatives of the hydroperoxide lyase pathway are produced by product recycling through lipoxygenase-2 in *Nicotiana attenuata* leaves. N. Phytol. 191, 1054–1068. https://doi.org/10.1111/j.1469-8137.2011.03767.x.

Kamaruddin, H.S., Megawati, M., Nurliana, N., Sabandar, C.W., 2021. Chemical constituents and antioxidant activity of *Melothria scabra* naudin fruits. Borneo J. Pharm. 4, 283–292. https://doi.org/10.33084/bjop.v4i4.2890.

Khan, R.A.A., Najeeb, S., Chen, J., Wang, R., Zhang, J., Hou, J., Liu, T., 2023. Insights into the molecular mechanism of *Trichoderma* stimulating plant growth and immunity against phytopathogens. Physiol. Plant 175, e14133. https://doi.org/10.1111/ppl.14133.

Kubiak, A., Wolna-Maruwka, A., Pilarska, A.A., Niewiadomska, A., Piotrowska-Cyplik, A., 2023. Fungi of the *Trichoderma* genus: future perspectives of benefits in sustainable agriculture. Appl. Sci. 13, 6434. https://doi.org/10.3390/app13116434.

Lana, M., Simón, O., Velasco, P., Rodríguez, V.M., Caballero, P., Poveda, J., 2023. First study on the root endophytic fungus *Trichoderma hamatum* as an entomopathogen: development of a fungal bioinsecticide against cotton leafworm (*Spodoptera littoralis*). Microbiol. Res. 270, 127334. https://doi.org/10.1016/j.micres.2023.127334.

Liu, Y., Wang, W., Ren, G., Cao, Y., Di, J., Wang, Y., Zhang, L., 2024. Selenium treatment regulated the accumulation of reactive oxygen species and the expressions of related genes in postharvest broccoli. Agronomy 14, 1047. https://doi.org/10.3390/agronomy14051047.

Livak, K.J., Schmittgen, T.D., 2001. Analysis of relative gene expression data using real-time quantitative PCR and the $2^{-\Delta\Delta CT}$ method. Methods 25, 402–408. https://doi.org/10.1006/meth.2001.1262.

Lodi, R.S., Peng, C., Dong, X., Deng, P., Peng, L., 2023. *Trichoderma hamatum* and its benefits. J. Fungi 9, 994. https://doi.org/10.3390/jof9100994.

Lombardi, N., Vitale, S., Turrà, D., Reverberi, M., Fanelli, C., Vinale, F., et al., 2018. Root exudates of stressed plants stimulate and attract *Trichoderma* soil fungi. Mol. Plant. Microbe Inter. 31, 982–994. https://doi.org/10.1094/MPMI-12-17-0310-R.

Lovelock, D.A., Donald, C.E., Conlan, X.A., Cahill, D.M., 2013. Salicylic acid suppression of clubroot in broccoli (*Brassicae oleracea* var. *italica*) caused by the obligate biotroph *Plasmodiophora brassicae*. Australas. Plant Pathol. 42, 141–153. https://doi.org/10.1007/s13313-012-0167-x.

Macioszek, V.K., Jęcz, T., Ciereszko, I., Kononowicz, A.K., 2023. Jasmonic acid as a mediator in plant response to necrotrophic fungi. Cells 12, 1027. https://doi.org/10.3390/cells12071027.

Morcuende, J., Martín-García, J., Velasco, P., Sánchez-Gómez, T., Santamaría, Ó., Rodríguez, V.M., Poveda, J., 2024. Effective biological control of chickpea rabies (*Ascochyta rabiei*) through systemic phytochemical defenses activation by *Trichoderma* roots colonization: from strain characterization to seed coating. Biol. Control 193, 105530. https://doi.org/10.1016/j.biocontrol.2024.105530.

Moreira, X., Granjel, R.R., de la Fuente, M., Fernández-Conradi, P., Pasch, V., Soengas, P., et al., 2021. Apparent inhibition of induced plant volatiles by a fungal pathogen prevents airborne communication between potato plants. Plant Cell Environ. 44, 1192–1201. https://doi.org/10.1111/pce.13961.

Nicolás, C., Calvo-Polanco, M., Poveda, J., Alonso-Ramírez, A., Ascaso, J., Arbona, V., Hermosa, R., 2024. The presence of arbuscular mycorrhizal fungi in the rhizosphere of transgenic rapeseed overexpressing a *Trichoderma Thkel1* gene improves plant development and yield. Agriculture 14, 851. https://doi.org/10.3390/agriculture14060851.

O'Sullivan, C.A., Belt, K., Thatcher, L.F., 2021. Tackling control of a cosmopolitan phytopathogen: *Sclerotinia*. Front Plant Sci. 12, 707509. https://doi.org/10.3389/fpls.2021.707509.

Oelmüller, R., 2019. Interplant communication via hyphal networks. Plant Physiol. Rep. 24, 463–473. https://doi.org/10.1007/s40502-019-00491-7.

Poveda, J., 2020. *Marchantia polymorpha* subsp. *ruderalis* (Bischl. and Boissel.-Dub.)-arbuscular mycorrhizal fungi interaction: beneficial or harmful? Symbiosis 82, 165–174. https://doi.org/10.1007/s13199-020-00708-6.

Poveda, J., 2021. Glucosinolates profile of *Arabidopsis thaliana* modified root colonization of *Trichoderma* species. Biol. Control 155, 104522. https://doi.org/10.1016/j.biocontrol.2020.104522.

Poveda, J., 2022. Effect of volatile and non-volatile metabolites from *Leptosphaeria maculans* on tomato calli under abiotic stresses. Plant Stress 3, 100054. https://doi.org/10.1016/j.stress.2021.100054.

Poveda, J., Abril-Urías, P., Muñoz-Acero, J., Nicolás, C., 2023b. A potential role of salicylic acid in the evolutionary behavior of *Trichoderma* as a plant pathogen: from *Marchantia polymorpha* to *Arabidopsis thaliana*. Planta 257, 6. https://doi.org/10.1007/s00425-022-04036-5.

Poveda, J., Calvo, J., Barquero, M., González-Andrés, F., 2022. Activation of sweet pepper defense responses by novel and known biocontrol agents of the genus *Bacillus* against *Botrytis cinerea* and *Verticillium dahliae*. Eur. J. Plant Pathol. 164, 507–524. https://doi.org/10.1007/s10658-022-02575-x.

Poveda, J., Hermosa, R., Monte, E., Nicolás, C., 2019. The *Trichoderma harzianum* Kelch protein ThKEL1 plays a key role in root colonization and the induction of systemic defense in Brassicaceae plants. Front. Plant Sci. 10, 1478. https://doi.org/10.3389/fpls.2019.01478.

Poveda, J., Rodríguez, V.M., Abilleira, R., Velasco, P., 2023a. *Trichoderma hamatum* can act as an inter-plant communicator of foliar pathogen infections by colonizing the roots of nearby plants: a new inter-plant "wired communication. Plant Sci. 330, 111664. https://doi.org/10.1016/j.plantsci.2023.111664.

Poveda, J., Zabalgogeazcoa, I., Soengas, P., Rodríguez, V.M., Cartea, M.E., Abilleira, R., Velasco, P., 2020. *Brassica oleracea* var. *acephala* (kale) improvement by biological activity of root endophytic fungi. Sci. Rep. 10, 20224. https://doi.org/10.1038/s41598-020-77215-7.

Pozo, M.I., Herrero, B., Martín-García, J., Santamaría, Ó., Poveda, J., 2024. Evaluating potential side effects of *Trichoderma* as biocontrol agent: a two-edges sword? Curr. Opin. Environ. Sci. Health 41, 100566. https://doi.org/10.1016/j.coesh.2024.100566.

Rhoades, D.F., 1983. Responses of alder and willow to attack by tent caterpillars and webworms: evidence for pheromonal sensitivity of willows. Am. Chem. Soc. Symp. Ser. 208, 55–68. https://doi.org/10.1021/bk-1983-0208.ch004.

Rillig, M.C., Lehmann, A., Mounts, I.R., Bock, B.M., 2025. Concurrent common fungal networks formed by different guilds of fungi. N. Phytol. 246, 33. https://doi.org/10.1111/nph.20418.

Rubel, M.H., Abuyusuf, M., Nath, U.K., Robin, A.H.K., Jung, H.J., Kim, H.T., et al., 2020. Glucosinolate profile and glucosinolate biosynthesis and breakdown gene expression manifested by black rot disease infection in cabbage. Plants 9, 1121. https://doi.org/10.3390/plants9091121.

Sánchez-Gómez, T., Martín-García, J., Santamaría, Ó., Poveda, J., 2025. Improvement of oilseed *Brassica* crops by *Trichoderma* use: gene transfer and direct interaction. Oil Crop Sci. 10, 51–63. https://doi.org/10.1016/j.ocsci.2025.02.001.

Shang, Q., Jiang, D., Xie, J., Cheng, J., Xiao, X., 2024. The schizotrophic lifestyle of *Sclerotinia sclerotiorum*. Mol. Plant Pathol. 25, e13423. https://doi.org/10.1111/mpp.13423.

Sharifi, R., Jeon, J.S., Ryu, C.M., 2022. Belowground plant–microbe communications via volatile compounds. J. Exp. Bot. 73, 463–486. https://doi.org/10.1093/jxb/erab465.

Sharifi, R., Ryu, C.M., 2021. Social networking in crop plants: Wired and wireless cross-plant communications. Plant Cell Environ. 44 (4), 1095–1110. https://doi.org/10.1111/pce.13966.

Simard, S.W., 2018. Mycorrhizal networks facilitate tree communication, learning, and memory. Memory and Learning in Plants. Springer, Cham, pp. 191–213.

Singh, S.P., Keswani, C., Singh, S.P., Sansinenea, E., Hoat, T.X., 2021. *Trichoderma* spp. mediated induction of systemic defense response in brinjal against *Sclerotinia sclerotiorum*. Curr. Res. Microb. Sci. 2, 100051. https://doi.org/10.1016/j.crmicr.2021.100051.

Singh, A., Satheeshkumar, P.K., 2025. Plant communication: how plants converse and cope up. Bot. Rev. 91, 286–330. https://doi.org/10.1007/s12229-025-09316-9.

Šmilauer, P., Košnar, J., Kotilínek, M., Šmilauerová, M., 2020. Contrasting effects of host identity, plant community, and local species pool on the composition and colonization levels of arbuscular mycorrhizal fungal community in a temperate grassland. N. Phytol. 225, 461–473. https://doi.org/10.1111/nph.16112.

Torres-Contreras, A.M., Senes-Guerrero, C., Pacheco, A., González-Agüero, M., Ramos-Parra, P.A., Cisneros-Zevallos, L., Jacobo-Velazquez, D.A., 2018. Genes differentially expressed in broccoli as an early and late response to wounding stress. Postharvest Biol. Technol. 145, 172–182. https://doi.org/10.1016/j.postharvbio.2018.07.010.

Vahabi, K., Reichelt, M., Scholz, S.S., Furch, A.C., Matsuo, M., Johnson, J.M., et al., 2018. *Alternaria brassicae* induces systemic jasmonate responses in *Arabidopsis* which travel to neighboring plants via a *Piriformsopora indica* hyphal network and activate abscisic acid responses. Front. Plant Sci. 9, 626. https://doi.org/10.3389/fpls.2018.00626.

Velasco, P., Abilleira, R., Díaz-Urbano, M., Poveda, J., 2026. A novel mechanism of plant defense induction by *Trichoderma hamatum* via cell wall-derived elicitors from *Sclerotinia sclerotiorum*. Plant Soil.

Velasco, P., Rodríguez, V.M., Soengas, P., Poveda, J., 2021. *Trichoderma hamatum* increases productivity, glucosinolate content and antioxidant potential of different leafy brassica vegetables. Plants 10, 2449. https://doi.org/10.3390/plants10112449.

Wang, X., Wang, S., Basit, A., Wei, Q., Zhao, K., Liu, F., Zhao, Y., 2025. Metabolomics provides new insights into the mechanisms of *Wolbachia*-induced plant defense in cotton mites. Microorganisms 13, 608. https://doi.org/10.3390/microorganisms13030608.

Wen, T., Zhao, M., Yuan, J., Kowalchuk, G.A., Shen, Q., 2021. Root exudates mediate plant defense against foliar pathogens by recruiting beneficial microbes. Soil Ecol. Lett. 3, 42–51. https://doi.org/10.1007/s42832-020-0057-z.

Yi, G.E., Robin, A.H.K., Yang, K., Park, J.I., Hwang, B.H., Nou, I.S., 2016. Exogenous methyl jasmonate and salicylic acid induce subspecies-specific patterns of glucosinolate accumulation and gene expression in *Brassica oleracea* L. Molecules 21, 1417. https://doi.org/10.3390/molecules21101417.

Zamani-Noor, N., Hornbacher, J., Comel, C.J., Papenbrock, J., 2021. Variation of glucosinolate contents in clubroot-resistant and-susceptible *Brassica napus* cultivars in response to virulence of *Plasmodiophora brassicae*. Pathogens 10, 563. https://doi.org/10.3390/pathogens10050563.